

MAGNETISM & MAGNETIC MATERIALS

High-Field Magnetization and Exchange Interactions in $\text{Sn}_{1-x}\text{Gd}_x\text{Te}$

Anderson, J.R., Univ. of Maryland, Physics
Górska, M., Institute of Physics, Warsaw, Poland
Wolters, C., NHMFL*

We report preliminary results from vibrating-sample-magnetization (VSM) investigations of the diluted magnetic semiconducting (DMS) material, $\text{Sn}_{1-x}\text{Gd}_x\text{Te}$. Measurements have been carried out, in some cases to 31 T, with the high-field, water-cooled resistive magnet (cell 12) at NHMFL.

It has been hypothesized that the exchange interaction in this DMS system should depend upon the carrier concentration¹ and possibly upon the concentration of Gd, as was the case for Eu in $\text{Pb}_{1-x}\text{Eu}_x\text{Te}$.² In order to search for such dependences, three different values of x were selected, from Bridgman-grown crystals, and the carrier concentrations were modified by annealing in Sn vapor. The x -values, carrier concentrations, and magnetization parameters are shown in Table 1.

Table 1. $\text{Sn}_{1-x}\text{Gd}_x\text{Te}$ parameters.

x_{nom}	anneal ^a	p^b (10^{20}cm^{-3})	x_s^c	x_p^d	J_p/k_B^e (K)
0.025	u	8.3	0.017	0.015	-0.4
0.025	a	7.2	0.010	0.015	-0.9
0.04	u	5.9	0.02	0.019	-0.5
0.04	a	3.1	0.007	0.035	-1.1
0.06	u	5.6	0.028	0.053	-0.9
0.06	a	0.9	0.04	0.07	-0.4

^a u-unannealed; a-annealed

^b hole concentration from Hall effect measurements

^c isolated magnetic-ion concentration

^d pair contribution

^e J_p is the pair exchange and k_B is Boltzmann's constant.

Since the as-grown hole concentration results from Sn vacancies, it is not surprising that the hole concentration is reduced by annealing.

In Figure 1 we show representative magnetization data at 1.3 K for the annealed samples with three different compositions. There is more noise in the uppermost curve because the sample mass was much smaller than that of the other two. All the data have been fitted to an expression for the magnetization of single ions and pairs.² We expect the sum of x_s and x_p to be approximately the same as x_{nom} , which was

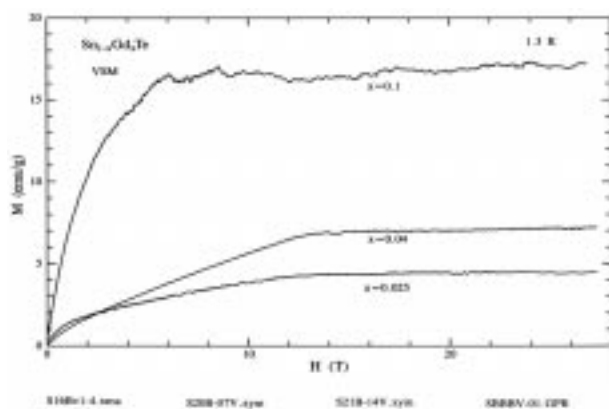


Figure 1. Magnetization vs. field for annealed $\text{Sn}_{1-x}\text{Gd}_x\text{Te}$ with x values 0.025, 0.04, and 0.1.

estimated from the growth conditions. For $x_{\text{nom}}=0.06$ this is not the case and, since we believe the value from the magnetization is more reliable, we have labeled this curve $x=0.1$ in Figure 1.

The parameters in Table 1 are the results of averages of several field sweeps at two temperatures, 1.3 K and 4.2 K. The final column in Table 1 shows the pair exchange values. For the smaller compositions we find, as expected, that the magnitude of the exchange is greater for the smaller carrier concentration. For the largest x -value, however, we find the opposite. It may be that the carrier density in this last annealed sample is too low to promote the resonance exchange mechanism,¹ but our study is not yet complete.

Other experiments on the same $\text{Sn}_{1-x}\text{Gd}_x\text{Te}$ system with the cantilever system at dilution refrigerator temperatures showed de Haas-van Alphen oscillations and features that may represent magnetization steps. These results will be reported later.

* Present address: KLA-Tencor, 5 Technology Drive, Milpitas, CA 95035.

References:

- ¹ Story, T., *et al.*, Acta Physica Polonica, **A90**,935 (1996).
- ² Górska, M., *et al.*, Phys. Rev., **B55**, 4400 (1997).

Dynamical Properties of the Spin-Peierls Compound NaV_2O_5

Augier, D., Lab de Physique Quantique, Toulouse, France

Poiblanc, D., Lab de Physique Quantique, Toulouse, France

Haas, S., ETH, Zurich, Switzerland

Delia, A., NHMFL

Dagotto, E., FSU, Physics/NHMFL

Dynamical properties of the inorganic spin-Peierls compound NaV_2O_5 are investigated using a one-dimensional dimerized Heisenberg model. By exact diagonalization of chains with up to 28 sites, supplemented by finite-size scaling analysis, the dimerization parameter is determined by requiring that the model reproduce the experimentally observed spin-gap. The dynamical and static spin structure factors are calculated. As for CuGeO_3 , the existence of a low-energy magnon branch separated from the continuum is predicted. The present calculations also suggest that a large magnetic Raman scattering intensity should appear above an energy threshold of 1.9 times the gap. The predicted photoemission spectrum is qualitatively similar to results for an undimerized chain due to the presence of sizable short-range antiferromagnetic correlations.¹

References:

- ¹ Augier, D., *et al.*, Phys. Rev., **56**, R5732 (1997).

1.20 GHz to 330 GHz Frequency Dependence of the EPR Linewidth of the S=1/2 Heisenberg Antiferromagnet K₃CrO₈: A Comprehensive Test of the Anderson-Weiss Model

Cage, B., NHMFL/FSU, Chemistry

Cevc, P., J. Stefan Institute, Univ. of Ljubljana, Slovenia

Blinc, R., J. Stefan Institute, Univ. of Ljubljana, Slovenia

Brunel, L.-C., NHMFL/FSU, Physics

Dalal, N., NHMFL/FSU, Chemistry

We have performed systematic single crystal EPR linewidth measurements spanning the range from 1.20 GHz to 330 GHz for simple S = 1/2, I = 0 systems. For example, as shown in Figure 1, the linewidth of the K₃CrO₈ single crystal shows an unambiguous Anderson-Weiss¹ type narrowing as the observation frequency exceeds the exchange frequency, and then an anomalous broadening that is not explained by "g-strain" or instrumental factors up to 330 GHz.

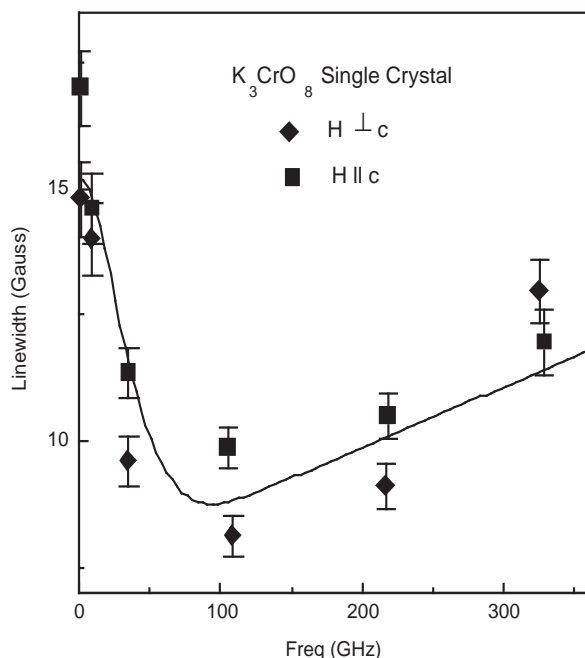


Figure 1. The EPR linewidth as a function of frequency of K₃CrO₈ for the crystal c axis parallel and perpendicular to the Zeeman field.

The experimental data could be well simulated by a modified equation (Eq. 1) based on Anderson-Weiss theory (solid line).

$$\Delta H_{\text{int}} = \frac{H_p^2}{H_{\text{ex}}} \left[1 + \frac{5}{3} e^{-\left(\frac{\omega}{\omega_0}\right)^2} + \frac{2}{3} e^{-\left(\frac{\omega}{\omega_0}\right)^4} \right] \cdot \omega_0 X + \omega_0 X + \text{Constant}$$

Excessive broadening at the higher frequencies is tentatively attributed to other interactions such as signal spitting from non-equivalent g-tensors. These results help understand the enhancement of resolution at higher fields of the EPR signal from concentrated spin 1/2 paramagnets.²

References:

- 1 Anderson, P.W., *et al.*, Rev. Mod. Phys., **25**, 1 (1953).
- 2 Cage, B., *et al.*, J. Magn. Reson., **124**, 495 (1997).

Detection of a Second Order Phase Transition in a Chromium (V) Compound Using Magnetization, Specific Heat and High Field EPR

Cage, B., FSU, Chemistry/NHMFL

McCall, S., NHMFL

Pardi, L., NHMFL

Singh, K., FSU, Chemistry

Cao, G., NHMFL

Crow, J.C., NHMFL

Brunel, L.-C., NHMFL

Dalal, N., FSU, Chemistry/NHMFL

We have used the combination of specific heat, magnetization and high field EPR measurements to gain complementary details about phase transitions. For instance, the existence of a second order phase transition in the model compound Na₃CrO₈ is indicated by a specific heat vs. temperature plot that shows a sharp lambda type peak at 2.2 K. Magnetic susceptibility measurements indicate antiferromagnetic ordering in the same region.

The superior resolution of the g-tensors by EPR at high magnetic fields allows the determination of the electronic ground state.¹ The observation of a change in ground state can confirm and elucidate the nature of a transition. For a tetrahedral system if $g_z < g_y < g_x$ (where g is the g-tensor, and the higher the g-value the lower the resonance field) then the ground state is $d_{(x^2-y^2)}$ while if $g_z > g_y > g_x$ then the ground state is d_{z^2} . The figure below shows the shift of the g_z resonance from the high field side to the low field side of the spectrum as the temperature is changed from 3.3 K to 1.4 K. This dramatic change in ground state could be indicative of a long range ordering of the crystal structure, and further studies with neutron diffraction could help confirm the nature of this transition.

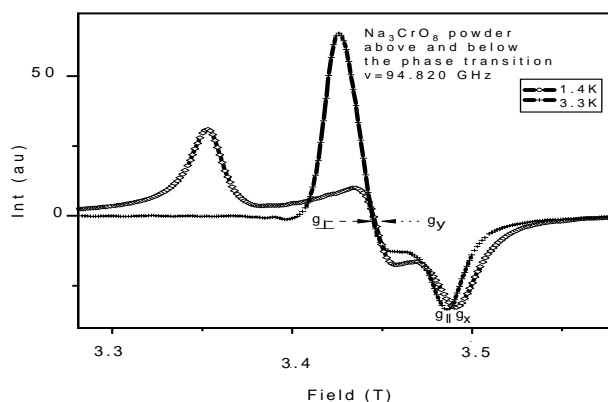


Figure 1. EPR spectra of Na_3CrO_8 at 3.3 K and 1.4 K.

References:

1. Cage, B., *et al.*, J. Magn. Reson., **124**, 495-98 (1997).

Physical Properties of Layered Ruthenates and Iridates

Cao, G., NHMFL
McCall, S., NHMFL
Shepard, M., NHMFL
Crow, J.E., NHMFL
Guertin, R.P., Tufts Univ., Physics

In the 1996 NHMFL report, this group presented an outline of the physical properties of a sequence of single crystal ruthenium-based oxides, all of which fall into the Ruddlesden-Popper sequence,

$(\text{Sr,Ca})_{n+1}\text{Ru}_n\text{O}_{3n+1}$ where $n = 1$ to ∞ and represents the number of repeated layers in a Ru-O layered sequence. Many of these materials were synthesized and characterized first in the NHMFL laboratories, and they are currently in high demand by other groups capable of performing specialized measurements. The phase diagram, shown in Figure 1, is much more complete based on work in the past year, and for the first time the $n = 3$ member was synthesized, $\text{Sr}_4\text{Ru}_3\text{O}_{10}$, with ferromagnetic properties consistent with the $n = 2$ and $n = \infty$ members in the sequence. The low temperature electronic specific heat coefficients are also shown. Nearly every magnetic phase is represented in this sequence or in stoichiometric mixtures of the components of the sequence. The pseudoternary series $(\text{Sr}_{1-x}\text{Ca}_x)\text{RuO}_3$ for $0 \leq x \leq 1.0$ shows a smooth evolution from ferromagnetism ($T_c = 165$ K for $x = 0$) to very highly enhanced paramagnetism for $x = 1.0$, where minute substitution of Sr for Ca produces spin-glass like behavior. The evolution of the electronic specific heat coefficient, Hall effect, and magnetic anisotropy are non-monotonic. More complex phases are found for another series $(\text{Sr}_{1-x}\text{Ca}_x)_3\text{Ru}_2\text{O}_7$, ranging from ferromagnetism ($x = 0$) to complex

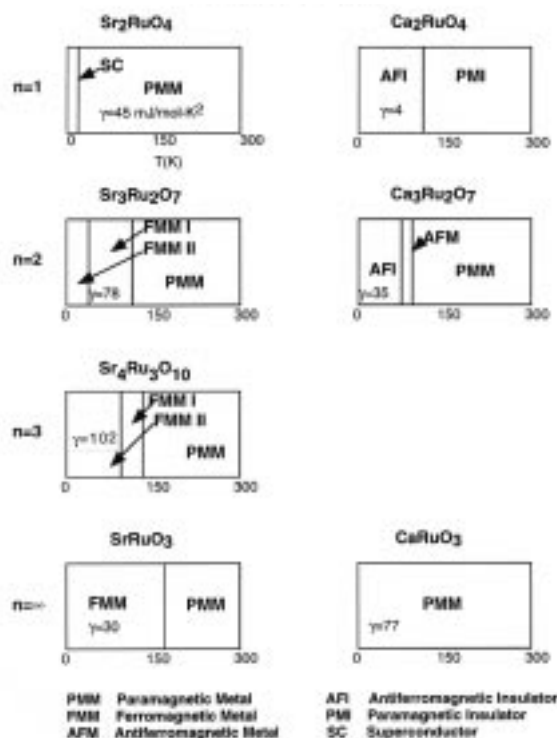


Figure 1. Phase diagram of $(\text{Sr,Ca})_{n+1}\text{Ru}_n\text{O}_{3n+1}$.

antiferromagnetism ($x = 1.0$). In spite of all this complexity, strong trends are noted in the ordering temperatures: T_C increases from $n = 1$ to $n = \infty$ for Sr-based and T_N (Neel temperature) decreases for Ca-based compounds. This is illustrated in Figure 2.

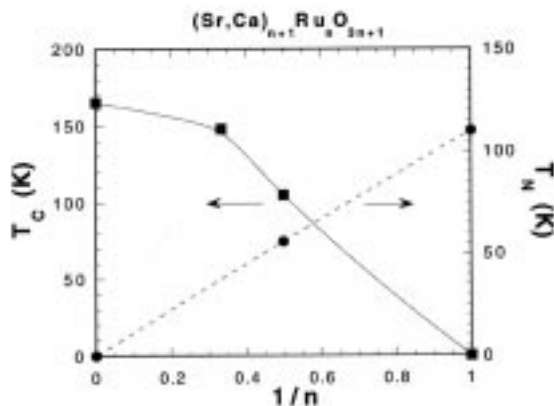


Figure 2. Curie and Neel temperature vs. $1/n$, n is the number of layers. The squares represent Sr-based and circles Ca-based systems.

Recent efforts have succeeded in synthesizing some single crystal Ir-based (5d) systems, Sr_2IrO_4 , BaIrO_3 and CaIrO_3 . They tend to be less metallic, and the moments associated with each Ir are very small ($\approx 0.03 \mu_B/\text{Ir}$) far less than expected for the low spin state of Ir, but the magnetic ordering temperatures are high. Sr_2IrO_4 represents the $n = 1$ member of the R-P iridate sequence that will be completed at least for $n = 1, 2$ and ∞ in the coming year.

Intergrain Effects on the Colossal Magnetoresistance in Polycrystalline $\text{Pr}_{1-x}\text{Ba}_x\text{MnO}_3$

Cohenca, C.H., USP-Brazil, Physics

Jardim, R.F., USP-Brazil, Physics

Torikachvili, M.S., San Diego State Univ., Physics

Lacerda, A.H., NHMFL/LANL

At the NHMFL-LANL we have studied the effect of contributions arising from intergrain on the electronic transport and general magnetic properties of $\text{Pr}_{1-x}\text{Ba}_x\text{MnO}_3$ for $0 < x < 0.45$. Polycrystalline samples of these compounds have

been produced using two different precursors: (1) mixture of the simple oxide Pr_6O_{11} and carbonates BaCO_3 , and MnCO_3 , and (2) using sol-gel precursors.¹ These samples were subject to heat treatment in air at 1100 C for $\sim 60\text{h}$. Observations of the microstructure and measurements of X-ray diffraction, electrical resistivity, magnetoresistivity, and magnetic susceptibility indicate the important effect that porosity and voids have upon the properties of these compounds. Samples prepared by using the sol-gel process are composed of small grains ($< 1\mu\text{m}$) and do not show any additional phase. Samples prepared with mixture of oxide and carbonates have larger grains and an additional Ba-rich phase BaMnO_3 . However, their macroscopic properties, as well as the colossal magnetoresistance, are almost insensitive to these differences. This suggests that intergrain effects must be taken into account to a better understanding of their properties.

References:

- Jardim, R.F., *et al.*, J. Alloys & Compounds, **199**, 105 (1993).

AFMR Study of $\text{KMnPO}_4 \cdot \text{H}_2\text{O}$ and a Series of Manganese Phosphonates

Fanucci, G.E., UF, Chemistry

Krystek, J., NHMFL

Meisel, M.W., UF, Physics

Brunel, L.-C., NHMFL

Talham, D.R., UF, Chemistry

Antiferromagnetic resonance (AFMR) is used to characterize the canted antiferromagnetic state and to probe magnetostructural correlations of a series of layered solids including $\text{KMnPO}_4 \cdot \text{H}_2\text{O}$, four alkylphosphonates, $\text{Mn}(\text{O}_3\text{PC}_n\text{H}_{2n+1}) \cdot \text{H}_2\text{O}$ $n = 3-6$, and manganese phenylphosphonate. All samples were investigated as powders. The high field electron magnetic resonance (EMR) facility at the NHMFL was used to acquire AFMR spectra. Source frequencies ranged from 24 GHz to 380

GHz and magnetic field range was 0 T to 14.5 T. For an orthorhombic antiferromagnet, three sharp peaks corresponding to three antiferromagnetic resonance modes, one parallel and two perpendicular to the magnetic easy-axis, can be observed simultaneously. Figure 1 shows AFMR spectra acquired for manganese pentylphosphonate at several frequencies. It is clear from this figure how the resonance field of each of the three signals changes as a function of source frequency. This dependence is depicted in Figure 2, which summarizes in the frequency and field plane the AFMR signals detected for $\text{KMnPO}_4 \cdot \text{H}_2\text{O}$. The data shown in Figure 2 were fit with the conventional mean-field theory of AFMR modified to include a Dzyaloshinsky-Moriya interaction, $H_{\text{D-M}}$, as a canting term.²

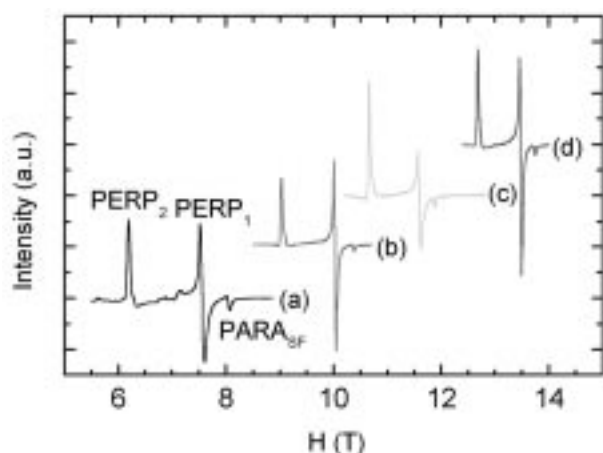


Figure 1. AFMR spectra detected for manganese pentylphosphonate at 5 K with source frequencies of (a) 218.18 GHz, (b) 285.42 GHz, (c) 330.37 GHz, and (d) 380.84 GHz.

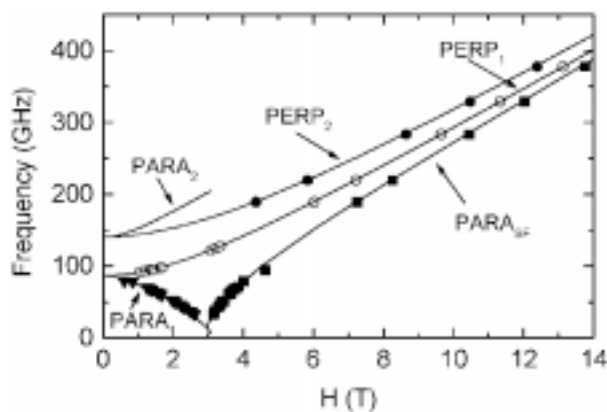


Figure 2. Frequency and field dependence of the AFMR signals detected for $\text{KMnPO}_4 \cdot \text{H}_2\text{O}$.

Fits to the data provided values for the in-plane magnetic exchange parameters for these materials, namely the symmetric isotropic exchange, H_E , the anisotropic exchange, H_{A1} and H_{A2} , and the Dzyaloshinsky-Moriya exchange, $H_{\text{D-M}}$. The trend in the value of H_E for each material followed the electron donating ability of the phosphate/phosphonate substituent. The Dzyaloshinsky-Moriya interaction, was found to be 0.3 T to 0.5 T \pm 0.2 T for these materials. The canting angle, β , defined as the angle that the sublattice magnetization vectors make with respect to the magnetic easy-axis, was determined to be 0.7-0.9° \pm 0.2° for all samples. The similarity of this angle in all the materials studied indicates that the degree of canting is not directly affected by changes in the phosphate/phosphonate substituents.

References:

- 1 Foner, S., *et al.*, in *Magnetism*; Academic Press, **1**, 383-447 (1963).
- 2 Moriya, T., Phys. Rev., **120**, 91-98 (1960).

Magnetic Properties of Zintl-Type Phases

Fisk, Z., NHMFL/FSU, Physics

Torelli, M., NHMFL/FSU, Physics

Petrovic, C., NHMFL/FSU, Physics

This research involves a study of Mn_5Si_3 -type hexagonal materials formed by Ce, Sm, and Yb. The motivation for this work was the result reported in the literature that $\text{La}_5\text{Si}_3\text{P}$ is a semiconductor. Our interest is in substituting for La other rare earths that have unstable valence, to see under what circumstances mixed valence develops.

The Mn_5Si_3 structure has two inequivalent Mn-sites, a three-fold one and a two-fold one. We have been preparing single crystals of rare earth 5-3's by flux growth from rare earth-first row transition metal eutectics, in particular with the elements Mn, Fe, Co, Ni, and Cu. The compounds have been with Si, Ge, Sn, and Pb on the Si sites. In general,

the crystals prepared are air sensitive, so that care needs to be taken to minimize their exposure to the atmosphere.

Our measurements have been primarily those of magnetic susceptibility, electrical resistivity along with x-ray characterization. Work that J.D. Corbett reported indicated that first row transition elements can be incorporated into anti-prisms formed by one of the La-sites in La_5Pb_3 , to form, for example $\text{La}_5\text{Pb}_3\text{Ni}$. Since we are using fluxes for the crystal growth that contain the first row transition metals, we expect that this incorporation might occur as well for our materials. This appears to be the case, as our extensive magnetic susceptibility studies indicate.

There are three primary issues here. The first is that the amount of incorporated transition metal is not necessarily one per formula unit, but appears in some cases to be two. Second, the flux element is not incorporated for all the elements used (Mn-Cu), and this also varies with which element in the Si column is used. And third, certain of the incorporated transition elements appear to carry a moment of their own.

Concerning this last observation, in the case where exactly one atom per formula unit is incorporated, these transition metal atoms form a linear array well separated from the closed parallel array. There are indications in the magnetic susceptibility that this chain undergoes some kind of magnetic order of its own at temperature of order 100 K, independent of the magnetic order that the rare earths show.

We also have evidence that the rare earths with unstable valence show in a number of cases heterogeneous mixed valence in this system: one of the sites has +3 rare earth, the other +2. Our current research is to understand exactly what determines this.

A New Probe to Perform Magneto-Optical Kerr Measurements on Thin Films and Multilayers

Geerts, W.,* UF, Materials Science and Engineering (MSE)/NHMFL

Childress, J., UF, MSE/NHMFL

Pearnton, S., UF, MSE/NHMFL

Schmiedel, T., NHMFL

Williams, V., NHMFL

A unique apparatus to measure the magneto-optical (MO) Kerr rotation and MO Kerr ellipticity of thin films and multilayers at high fields (0 T to 20 T) and low temperature (2 K to 325 K) was developed. With the realized equipment it is possible to determine the Kerr rotation with an accuracy better than 0.5 mdegree (10^{-8} 10^{-9} emu for iron). The residual background resulting from the Faraday rotation in the optical components, is smaller than 2 mdegree/T. A higher sensitivity and a lower background is obtained for the ellipticity signal. Typical sample diameters are between 0.5 cm and 2 cm. The equipment has been added to the user accessible instruments at the NHMFL facilities in Tallahassee.

The probe is built around a HINDS Photoelastic Modulator (PEM) and a HeNe laser. In order to avoid large contributions of the Faraday effect of air, the probe can be evacuated. Magnetic iron and μ -metal was used to shield the optics, i.e. lens (E), vacuum window (D), analyzer (G), polarizer (B), and PEM (C), from the magnetic stray field of the resistive magnet (see Figure 1). The lens-shield located at 1 m from the maximum field, has a total weight of 320 gram. The presence of these ferromagnetic materials close to the magnet required a rigid probe design in order to avoid field dependent bending of the probe by the magnetic stray field. The optimum shape (hollow tube) and one of the more rigid materials (stainless steel) did not provide sufficient rigidity. Extra constrictors between probe, vacuum can, and cryostat had to

be designed in order to obtain a sufficiently stiff construction.

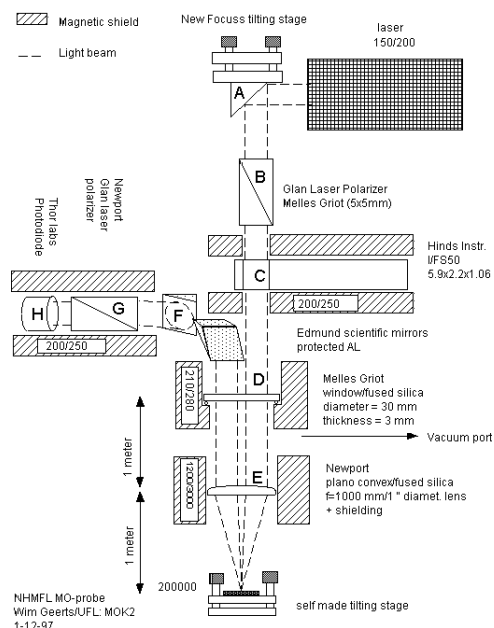


Figure 1. MOK3: a probe for high field low temperature magneto-optical Kerr measurements.

Measurements were performed on ultra thin epitaxial iron films sandwiched between gold. The results are shown in Figure 2. The iron has a thickness of 9 monolayers. The absence of hysteresis and the low noise level show the performance of this new probe.

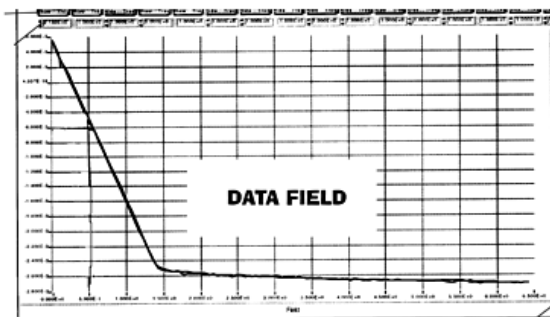


Figure 2. Polar MO Kerr hysteresis curve of 9 monolayers of Fe sandwiched between Au.

The authors would like to thank Dr. T. Katayama and Dr. Y. Suzuki of the Electrotechnical Laboratory in Tsukuba for providing the sample.

* Current address: Department of Physics, Southwest Texas State University, San Marcos, TX 78666.

Magneto-Optical Properties of FePt Epitaxial Films

Geerts, W.,* UF, Materials Science and Engineering (MSE)/NHMFL

Weller, D., IBM, Almaden Research Center, CA

Childress, J., UF, MSE/NHMFL

Pearton, S., UF, MSE/NHMFL

Thin film FePt alloys and multilayers are potential magneto-optic (MO) and magnetic recording materials. Recent studies show that epitaxial FePt alloy films grown near the equiatomic composition are chemically ordered. The fct FePt phase can be viewed as a natural superlattice with alternating monoatomic layers of Fe and Pt along the [001] direction. The ordered FePt has a large MO Kerr effect (a Kerr rotation of 0.9 degrees near 2 and 5 eV) and a huge magnetic anisotropy ($>7 \text{ MJ/m}^3$).^{1,2}

Figure 1 shows the polar MO Kerr spectra of epitaxial FePt films with two different orientations measured at a perpendicular field of 2.6 T (IBM data). As this field was too low to saturate the (110) films (see inset of Figure 1),

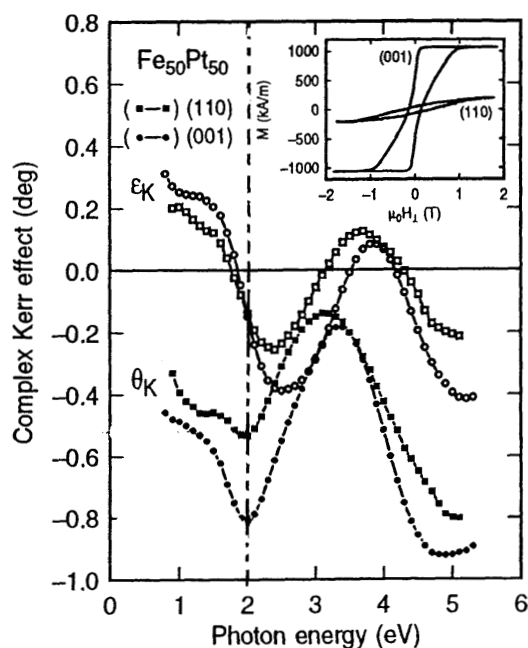


Figure 1. Polar Kerr rotation and Kerr ellipticity spectra of epitaxial FePt at 2.6 T.

the (110) spectra were scaled by a factor of four (based on the saturation magnetization of the sample).

In order to check the data of Figure 1, we performed high field MO experiments in Tallahassee.³ The measurements were done at 2 eV, for temperatures between 4 K and 300 K, in fields up to 20 T. Preliminary results are given in Figure 2. Remarkable is the hysteresis of the (110) oriented sample (up to 10 T). The saturation field appeared to increase with decreasing temperature. The measured values of the Kerr rotation and Kerr ellipticity in a field of 20 T are in agreement with the 2 eV data of Figure 1.

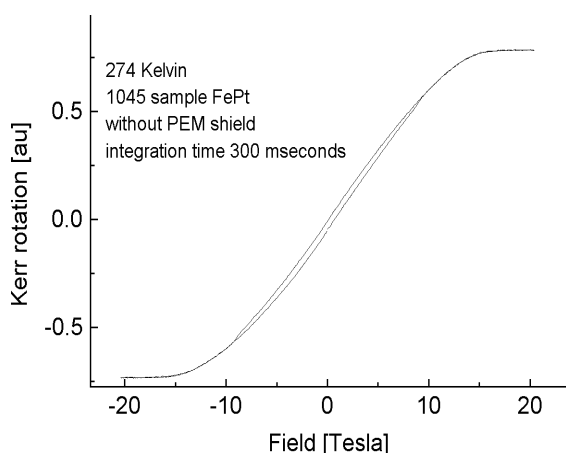


Figure 2. MO Hysteresis curve of epitaxial (110) FePT on MgO (110).

* Current address: Department of Physics, Southwest Texas State University, San Marcos, TX 78666.

References:

- 1 Cebollada, A, *et al.*, Phys. Rev. B, **50**, 3419 (1994).
- 2 Weller, D, in *Spin Orbit Influenced Spectroscopies of Magnetic Solids*, ISBN 3-540-60843-5, (Springer, 1996).
- 3 Geerts, W, MOK3: a high field magneto-optical Kerr probe, User Manual, NHMFL technical report (1997).

De Haas-van Alphen Measurements on EuB₆

Goodrich, R.G., Louisiana State Univ., Physics

Harrison, N., NHMFL

Vuillemin, J.J., Univ. of Arizona, Physics

Fisk, Z., NHMFL

Sarrao, J., NHMFL

We have taken temperature dependent pulsed field dHvA data on a sample of ferromagnetic EuB₆. An example of the oscillatory data from a down sweep plotted vs. $1/B$ is shown in Figure 1 with a small field region of both up and down sweep data shown in Figure 2. It is obvious that several low frequency dHvA oscillations are present in the data and from the inset it can be seen that they have the proper phase reversal for magnetization oscillations between up and down sweeps. The voltage induced in the coil by the oscillatory magnetization of the sample is given by

$$v_s = C'(dM/dB)(dB/dt),$$

and this changes sign with the changed sign of dB/dt between the up and down sweeps in a pulsed field experiment giving rise to the phase reversal in the oscillations.

After measuring the total magnetization of the same sample in the LSU SQUID magnetometer to give a starting point for determining the B field seen by the electrons in the sample, we make adjustments to the internal field for the dHvA

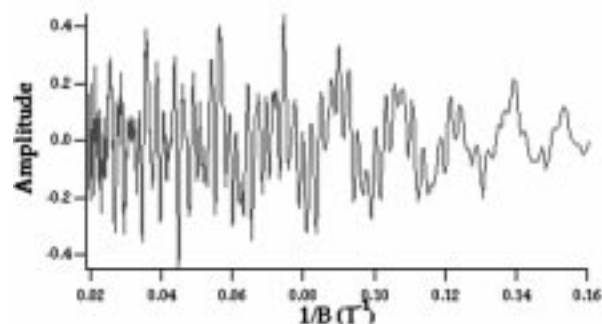


Figure 1. Magnetization as a function of reciprocal field in EuB₆ at T = 0.5 K.

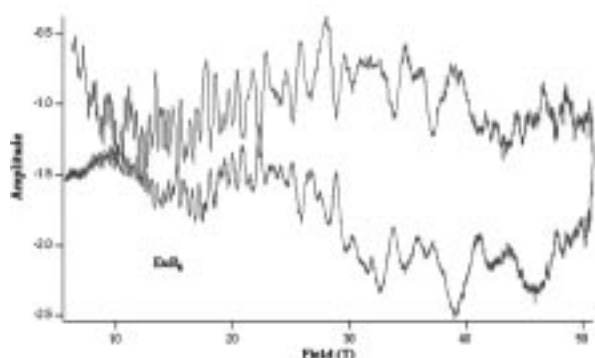


Figure 2. Magnetization of EuB_6 as a function of applied field for both increasing and decreasing fields.

measurements to maximize the amplitude and minimize the width of the peaks in the Fourier transform of the data. The final Fourier transform is shown in Figure 3. From this analysis we find definite dHvA oscillations were observed in the pulsed field data with four frequencies: 60 T ($m^* = 0.32$), 275 T ($m^* = 0.92$), 375 T ($m^* = 0.66$), and 575 T ($m^* = 0.75$). This is the first definitive observation of the FS of this material, and a paper is now being written.

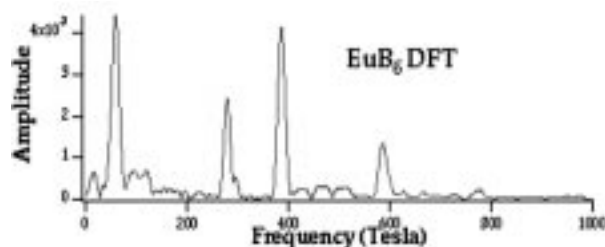


Figure 3. Fourier transform of the data shown in Figure 1, corrected for internal field.

Properties of Manganites

Gor'kov, L.P., NHMFL
Kresin, V.Z., Lawrence Berkeley Laboratory

There is a consensus that peculiar phenomenon of "Colossal Magnetoresistance" (CMR), in materials such as manganites, LaMnO_3 , doped by divalent elements, Ca or Sr, results from competition between the double exchange (DE) mechanism and the Jahn-Teller (JT) instability of degenerate outer electronic orbital, e.g., on Mn-ions. Correspondingly, the phase transition

at T^* , is treated in Reference 1 as a crossover between a regime in which electrons are localized by thermal fluctuations of the JT-distorted oxygen octahedrons, and onset of transport due to DE-mechanism.

This approach¹ is not helpful for understanding equilibrium low temperature properties of stoichiometric and lightly doped LaMnO_3 . Those most often are interpreted in terms of strongly correlated electrons (in a Hubbard model approach).

It is shown in Reference 2 that actually these properties follow directly from a band description, if both DE- and JT-mechanisms are properly taken into account. Namely, the antiferromagnetic (AF) ground state for LaMnO_3 results from the fact that a large Hund's coupling demands onset of AF-ordering along one direction, leading to alternating ferromagnetic layers. An AF-order along any other direction would be not capable to provide any further gain in the kinetic energy of electrons: JT-distortions are more effective by forming energy gaps in the electron's band spectrum. The unit cell becomes reduced both along the z-axis and in the plane. As the result, mere counting of available electronic states completes description of LaMnO_3 as a band insulator. Two dimensional (in the limit of large Hund's coupling) ferromagnetic layers are then responsible for further details.

As far as the transition between insulating and conducting states in doped manganites is concerned, we associated the value of the critical concentration, $x = 0.16$, with the threshold for percolation. Treatment of "CMR" as a percolation phenomena is currently studied in some more details.

References:

- 1 Millis, A., *et al.*, Phys. Rev. Lett., 77, 175 (1996).
- 2 Gor'kov, L.P., *et al.*, submitted to PRL (1997).

Magnetic Studies of End-Chain Spin Effects in the $S = 1$ Haldane Gap Material NINAZ

Granroth, G.E., UF, Physics
 Maegawa, S., UF, Physics
 Meisel, M.W., UF, Physics
 Ward, B.H., UF, Chemistry
 Chou, L.-K., UF, Chemistry
 Fanucci, G.E., UF, Chemistry
 Talham, D.R., UF, Chemistry
 Bell, N.S., UF, Materials Science and Engineering
 Adair, J.H., UF, Materials Science and Engineering
 Krzystek, J., NHMFL
 Brunel, L.-C., NHMFL

Magnetization and ESR studies on polycrystalline, powder, and ultrafine powder samples of the Haldane gap material known as NINAZ, $\text{Ni}(\text{C}_3\text{H}_{10}\text{N}_2)_2\text{N}_3(\text{ClO}_4)$, have revealed several novel effects.¹ For several reasons, NINAZ is an excellent model system for studying end-chain spins. Firstly, the nearest-neighbor interaction, J , is about 125 K,² and consequently, the Haldane gap $\Delta \approx 42$ K and the critical magnetic field $H_c \approx 30$ T. Consequently, $M(T = 2 \text{ K}, H \leq 5 \text{ T})$ and ESR ($T \leq 4 \text{ K}, H \leq 14 \text{ T}$) will probe the system that is deep in the Haldane phase. Secondly, the material has a structural transition, near 255 K, which naturally breaks the chains. Finally, additional chain breaks may be introduced by mechanically pulverizing the specimens, thereby eliminating the complications associated with chemically doping the chains.

Coupled with the determination of the g -value of the end-chain spin, $M(T = 2 \text{ K}, H \leq 5 \text{ T})$ data confirm that the end-chain spins are $S = 1/2$ and show no evidence for even/odd chain length effects.

The temperature dependence of the ESR intensity was fit to the expressions of Mitra, Halperin, and Affleck,³ providing a microscopic determination of the chain lengths. Comparisons of the chain lengths to the macroscopic particle size

distributions indicate that ball-milling may reduce the chains lengths below the lengths induced by the shattering process.

The line widths of the samples are significantly broader than expected from experimental conditions alone, Figure 1. The width of these lines has been interpreted within the model of Mitra, Halperin, and Affleck³ and show the first evidence of interactions between the excitations on the chains with the end-chain spins. This interaction involves a phase-shift of the magnetic excitation. To search for additional peaks associated with the excitations changing energy levels, high field ESR measurements were performed, but no additional structures were observed.

Additional studies of doped specimens of NINAZ are consistent with the present description, and a detailed report of the entire work is given elsewhere.⁴

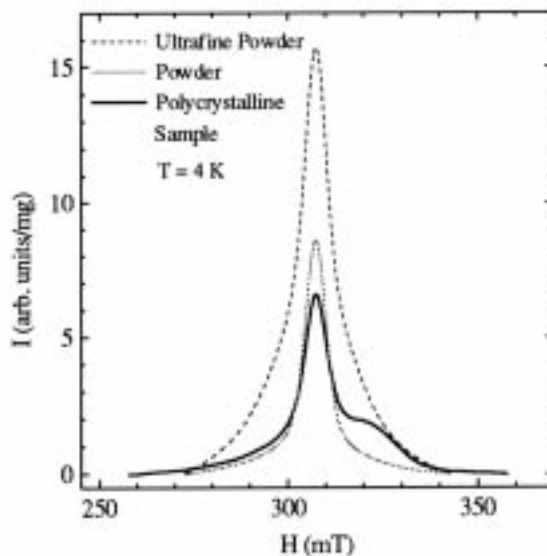


Figure 1. Typical 9 GHz ESR line shapes.

References:

- Granroth, G.E., *et al.*, LANL cond-mat/9710161.
- Zheludev, A., *et al.*, Phys. Rev. B, **53**, 15004 (1996).
- Mitra, P.P., *et al.*, Phys. Rev. B, **45**, 5299 (1992).
- Granroth, G.E., Ph.D. thesis, University of Florida (1998).

Current Controlled Negative Differential Resistivity in Ruthenates and Iridates

Guertin, R.P., Tufts Univ., Physics

Cao, G., NHMFL

Bolivar, J., NHMFL

McCall, S., NHMFL

Crow, J.E., NHMFL

The current-voltage characteristics of three examples of ternary ruthenium and iridium oxides show current controlled, or “S” shaped, negative differential resistivity (NDR) in the simple DC relationship between current and voltage. In all cases the effect appears only in the non-metallic phases of the materials, i.e., when the electrical resistivity, $\rho(T)$ increases with decreasing temperature, $d\rho(T)/dT < 0$. The first example of this effect is shown in the accompanying figure; in this case for single crystal $\text{Ca}_3\text{Ru}_2\text{O}_7$ a material with Ru-O bilayers separated by Ca-O layers that shows a variety of magnetic and transport properties as a function of temperature and magnetic field strength. The non-linear (non-Ohmic) I vs. V is confined to the antiferromagnetic insulating region of the field-temperature phase space, namely $0 < T < 48$ K and $0 < H < 6$ T, where here the field is along the easy axis direction and the temperature 48 K represents the first order insulator to metal transition. Very similar I - V characteristics are found for Sr_2IrO_4 and BaIrO_3 , both of which are non-metallic and which show weak ferromagnetic transitions at $T = 250$ K and 175 K, respectively. In “S” NDR the system is unstable to the development of a low resistance filamentary current structure, and differs from the Gunn or Esaki diode effect, which has “N” shaped I - V . To our knowledge these are the first examples of “S” NDR in 4d and 5d transition metal oxides, but we believe it may be pervasive among many of near metallic oxide materials being so assiduously investigated, but overlooked to date. The effect may be due to depinning of a charge density wave in these lower dimensional structures, interplane hopping, or perhaps a transferred electron effect between excited band states with differing mobility. Electronic devices

based on NDR include oscillators, amplifiers and even computer elements.

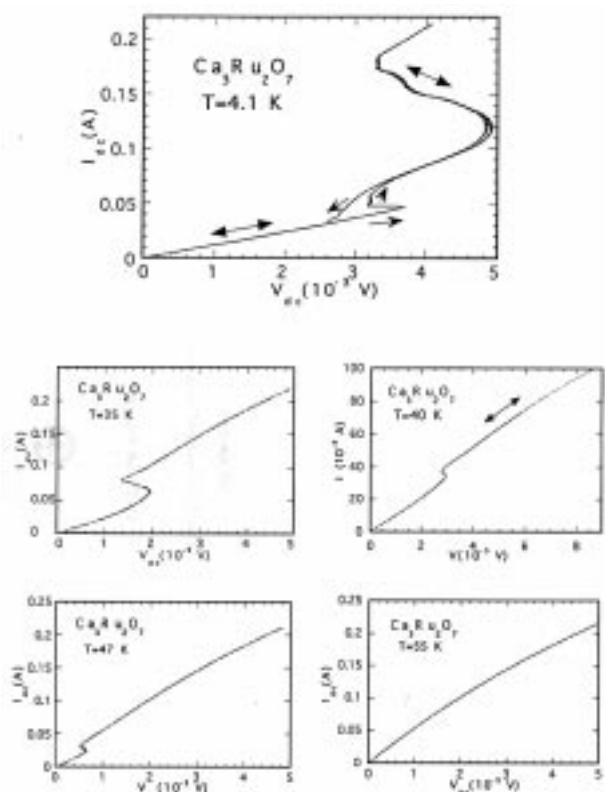


Figure 1. I - V curves for $\text{Ca}_3\text{Ru}_3\text{O}_7$.

New Paired-Wavefunction for the Frustrated Antiferromagnetic Spin-Half Chain

Ha, Z.N.C., NHMFL

I propose a new paired-wavefunction with a parameter that continuously interpolates from the 1D Jastrow-product to the Majumdar-Ghosh dimer-wavefunction appropriate for the frustrated Heisenberg $S = 1/2$ antiferromagnet. This spin paired-state constructed in S_z basis is an alternative to the well-known resonating-valence-bond basis state for describing the spin singlet ground-state with no apparent long-range spin order. Some numerical evidences are presented and further generalization to the 2D system in connection with the high T_c superconductors is in progress.

High Field ESR Studies of the Doped Spin-Peierls System CuGeO_3

Hassan, A.K., NHMFL/FSU, Physics
Pardi, L.A., NHMFL
Martins, G.B., NHMFL
Cao, G., NHMFL
Brunel, L.C., NHMFL

High field electron spin resonance (ESR) measurements were made on powder samples of the Zn doped Spin-Peierls system $\text{Cu}_{1-x}\text{Zn}_x\text{GeO}_3$ ($x=0.00, 0.01, 0.02, 0.03, 0.05$) at different frequencies (95, 110, 190, 220, 330 and 440 GHz) at low temperatures. The spectra of the doped samples show additional resonances relative to the spectra of the pure compound, whose positions are dependent on Zn concentration, frequency, and temperature. The analysis of the intensity behavior of these lines with temperature allows us to identify them as originating in transitions within states situated inside the Spin-Peierls gap. A qualitative explanation of the details of the spectra is possible if we assume that these states in the gap are associated with “loose” spins created near the Zn impurities, as recently theoretically predicted.¹ It is shown in Figure 1 that the experimental spectrum can be simulated as the sum of two individual

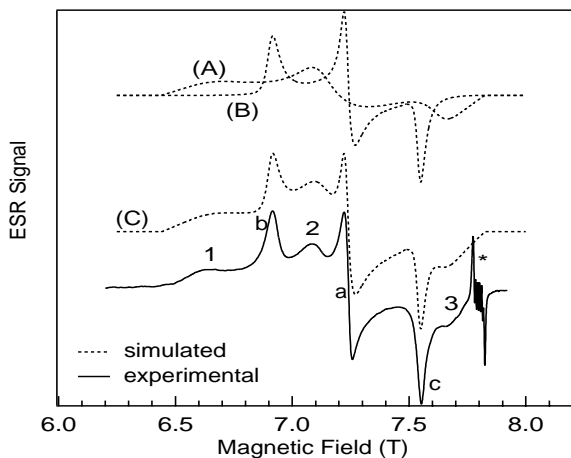


Figure 1. Experimental and simulated ESR spectra of the $x=0.02$ sample at 4.2 K and 218 GHz. Spectrum (C) is the sum of the individual spectra of the “loose” spins (A) and the “bulk” spins (B).

spectra, one for the “loose” spins and one for the “bulk” spins which coincides with the spectrum of the pure compound. We also observe that the original gap is partially suppressed upon doping. The ESR results presented here are the first observations of these states inside the gap. The behaviors of these excitations with temperature, frequency, and doping level offer an insight into the physical properties of the system investigated.

References:

- ¹ Martins, G.B., *et al.*, Phys. Rev. B, **54**, 16032 (1996).

Transport in Magnetic Nanostructures

Hershfield, S., UF, Physics/NHMFL

The phenomena called the Giant Magnetoresistance (GMR) occurs in materials composed of thin layers of magnetic and nonmagnetic metals. A relatively small field causes the magnetizations of the films to align, changing the resistance of the films by 50 percent or more. The giant magnetoresistance has gone from discovery to application in under a decade.

A natural question to ask is what happens if in addition to making thin films, one laterally confines the wires, e.g., makes layers of wires. With Kingshuk Majumdar and Jian Chen,¹ we have calculated the effect of laterally confining magnetic multilayers. The most generic result, shown in Figure 1, shows that the GMR decreases as one laterally confines the multilayers for the geometry where the current is in the plane of the multilayers. The origin of this decrease is that the effective mean free path in the layers is reduced due to scattering off the sides of the wires. We have found special cases where the GMR can increase with lateral confinement. These cases have strong spin dependent scattering at the interfaces. Fortunately, from an application point of view, the length scale for the GMR to be reduced is of order the mean

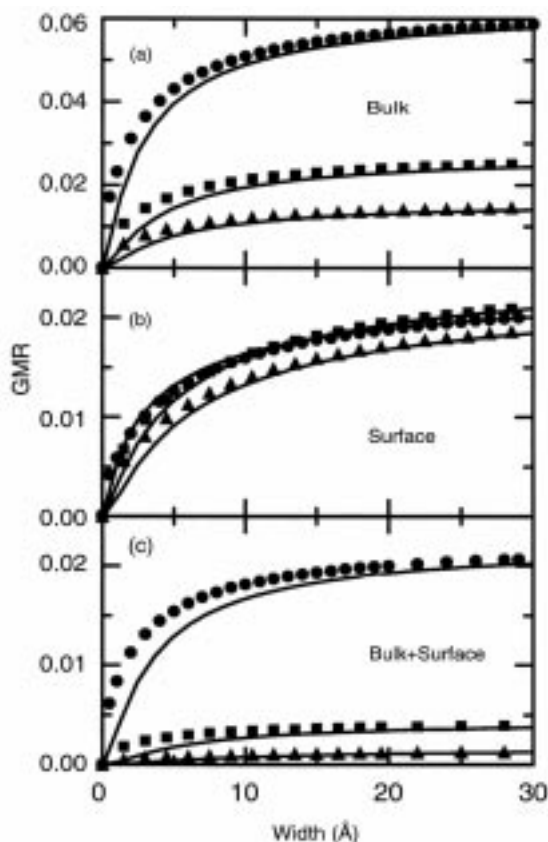


Figure 1. Giant magnetoresistance (GMR) of a three wire structure as a function of the width of the wires for different kinds of scattering: (a) bulk, (b) surface, and (c) bulk and surface. The parameters chosen for a Co/Cu/Co structure.

free paths in the films and the film thickness, which is quite small.

One can continue to confine the magnetic multilayers and go from layers of wires, which are one dimensional, to islands of magnetic materials, which are “zero dimensional” systems. With islands of magnetic and nonmagnetic metals separated by tunnel junctions one sees the phenomenon of the Coulomb blockade. The Coulomb blockade is seen when the charging energy of a pair of tunnel junctions is less than the temperature. Although it is based on the charge of an electron, there is spin and magnetic field dependence to the current-voltage characteristics for a system with of magnetic metals, like Ni or Fe. The spin dependence comes about because the tunneling rates depend on whether the magnetic metals are have magnetizations aligned parallel or antiparallel.

With Kingshuk Majumdar,² we have computed the magnetoresistance of a double junction system comprised of magnetic metals. A sample of curves for the junction magnetoresistance or JMR is shown in Figure 2.

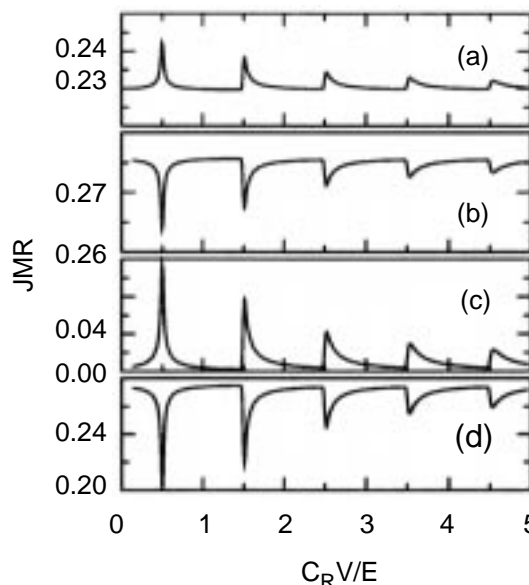


Figure 2. Junction magnetoresistance (JMR) as a function for voltage for a double barrier tunnel junction system in the following cases, when all of the metals are ferromagnetic (cases (a) and (b)), and when only two of the three components are ferromagnetic (cases (c) and (d)).

In addition to the above work, we have also examined the effects of spin-flip scattering on the GMR for current flowing in the planes of the multilayers and done microscopic quantum calculations of the GMR using realistic electronic structure.

References:

- ¹ Majumdar, K., *et al.*, to appear in Phys. Rev. B.
- ² Majumdar, K., *et al.*, submitted to Phys. Rev. B.

High Sensitivity EPR of Mn_{12} -Acetate

Hill, S., NHMFL

Perenboom, J.A.A.J., Univ. of Nijmegen, Physics

Dalal, N.S., NHMFL/FSU, Chemistry

Brooks, J.S., NHMFL/FSU, Physics

Stalcup, T., NHMFL/FSU, Physics

Hathaway, T., NHMFL/FSU, Chemistry

The Mn_{12} cluster complex, $[\text{Mn}_{12}\text{O}_{12}(\text{CH}_3\text{COO})_{16}(\text{H}_2\text{O})_4] \cdot 2\text{CH}_3\text{COOH} \cdot 4\text{H}_2\text{O}$, has attracted considerable interest due to indications that it exhibits the phenomenon of macroscopic quantum tunneling of magnetic moment (QTM). The cluster consists of four Mn(IV) ions, each with $S = 3/2$, surrounded by eight Mn(III) ions with $S = 2$. The clusters crystallize into a tetragonal lattice; the angular momentum is thought to be quenched, and a Jahn-Teller distortion produces a strong axial anisotropy. Superexchange leads to a high spin ground state where the spins of the Mn(IV) and Mn(III) ions are coupled parallel to $S = 6$ and $S = 16$ respectively; the spins of the outer shell are directed antiparallel to the spins of the inner ions. In the ground state, therefore, the cluster may be treated as an $S = 10$ object, with the spin preferentially aligned along the c -axis due to the axial anisotropy.

When the system is spin polarized by applying and removing a magnetic field ($B > 5$ T) parallel to the sample's easy axis, a sizable energy barrier inhibits the reversal of this moment ($\sim 64 k_B$). In spite of this, the spin system is somehow able to overcome this barrier at low temperatures. Below about 3 K, steps are observed in the hysteresis loop of oriented powder samples and single crystals.¹ The occurrence of these steps, at regularly spaced values of magnetic field, is seen as evidence that the magnetization reversal is due to QTM.

Until now, no single crystal EPR studies of Mn_{12} -Ac have been possible. We have used a multi-frequency, high-sensitivity EPR technique that enables us to make measurements on submillimeter sized single crystals. This is made possible by the use of resonant

cavities with resonance frequencies varying from 35 to 115 GHz. This frequency range allows us to probe the energy levels immediately below the top of the anisotropy barrier which, recent AC susceptibility measurements have indicated, may be crucial to the magnetization relaxation mechanism.

Figure 1 shows a compilation of all of the observed EPR transitions, versus in field,² over a fairly wide range of frequencies; the temperature is 35 K and the field is parallel to the sample's easy axis. The data are sufficiently detailed to make extremely accurate comparisons with predictions based on a spin $S = 10$ Hamiltonian.¹ Although overall agreement is good, we find evidence for possible inadequacies of this model.

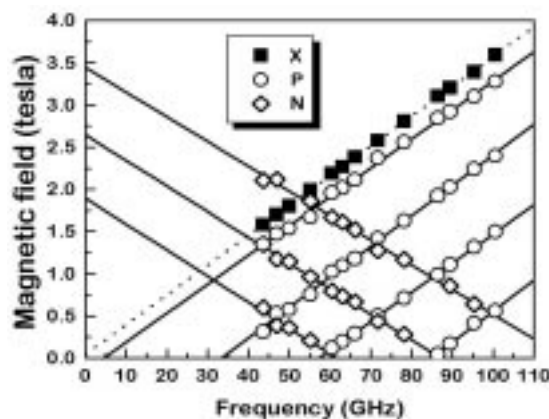


Figure 1. A compilation of the observed EPR transitions over a range of frequencies.

References:

- 1 Perenboom, J.A.A.J., *et al.*, submitted to Phys. Rev. B (August 1997).
- 2 Hill, S., *et al.*, submitted to Phys. Rev. Lett. (August 1997).

Magnetization of 1D and 2D Quantum Heisenberg Antiferromagnets

Landee, C.P., Clark Univ., Physics

Turnbull, M.M., Clark Univ., Chemistry

We are investigating the properties of several new families of low-dimensional $S = 1/2$ Heisenberg antiferromagnets with small exchange strengths

($2|J| = 1 - 15$ K) with the goal of understanding the influence of quantum effects upon the magnetic behavior.

A significant new family of antiferromagnetic linear chains is based upon the one-dimensional array of Cu^{2+} ions ($S = 1/2$) connected by pyrazine (pz) molecules, with the spacing between the chains provided by nitrate ions, $\text{Cu}(\text{pz})(\text{NO}_3)_2$. This compound is known to have a small exchange constant ($J/k = -5.3$ K,¹) and has recently become available in our laboratory as large single crystals. Replacing hydrogen atoms on the pyrazine ring by methyl groups has the effect of altering the exchange strength by as much as 50% without altering the chain structure. This family provides a framework in which to prepare quantum chains with random exchange interactions.²

We have begun our high-field studies with measurements of the magnetizations of three members of this family (Figure 1), using the NHMFL Vibrating Sample Magnetometer and a 30 T Bitter magnet. The data sets, collected at 2 K, show that the three compounds are saturated by approximately 15 T, 18 T, and 20 T, respectively, for the 2,3-dimethylpz, methylpz, and pure pz versions. The observed saturation fields are in good agreement with values predicted for the latter two

compounds using a molecular field model and the known exchange constants. The newly synthesized di-methyl compound demonstrates the range over which the exchange constant can be altered by chemical substitution.

References:

- 1 Losee, D.B., J. Chem. Phys., **59**, 3600 (1973).
- 2 Fisher, D.S., Phys. Rev. B, **50**, 3799 (1994).

High Temperature Hall Effect in Colossal Magnetoresistance Manganites

Lin, P., Univ. of Illinois at Urbana-Champaign, Physics
 Chun, S.-H., Univ. of Illinois at Urbana-Champaign, Physics
 Salamon, M.B., Univ. of Illinois at Urbana-Champaign, Physics
 Jaime, M., LANL
 Eckstein, J., Varian

Colossal magnetoresistance (CMR) manganites such as $\text{La}_{1-x}\text{Ca}_x\text{MnO}_3$ have been the subject of intense research during the last years, in part due to their potential use as device applications in the magnetic storage industry, and in part because of the complexity of the mechanisms responsible of unusual electric, magnetic and structural properties. It is believed that highly correlated electrons together with a significant lattice involvement in the form of a large electron-phonon interaction cooperate to induce a low temperature ferromagnetic metallic state, characterized by energy split up- and down-spin electronic bands. At high enough temperatures, on the other hand, the thermal entropy overcomes the exchange energy and the charge carriers lose their extended nature, self localizing into small polaronic states.

A remarkable consequence of the localization of these so called magneto-elastic polarons^{1,2} is the coincident paramagnetic-ferromagnetic and metal-semiconductor transitions at temperatures (T_c) close to room temperature. Resistivity,

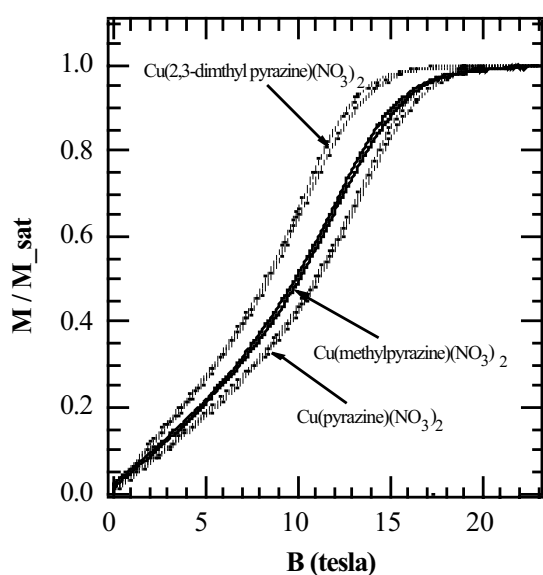


Figure 1. Relative magnetization curves of three isostructural $S = 1/2$ antiferromagnetic chains at 2 K.

thermoelectric power and Hall effect experiments performed on laser ablated films of composition $(\text{La}_{1-y}\text{Gd}_y)_{1-x}\text{Ca}_x\text{MnO}_3$ ^{1,3} were among the first pieces of experimental evidence supporting the polaronic interpretation. As a part of a program to improve our understanding of magnetoelastic polarons in CMR manganites, film samples of nominal composition $\text{La}_{0.9}\text{Sr}_{0.1}\text{MnO}_3$ were prepared by molecular beam epitaxy and patterned into a five contact geometry appropriate for a Hall effect experiment. Slightly different deposition conditions resulted in samples showing a range of T_c 's from 100 K to 300 K. Two of these samples (1442{2,1} $T_c = 260$ K and 1442{1,3} $T_c = 190$ K) were mounted in a specially designed variable-temperature-insert and placed inside a 20 T superconducting magnet at the NHMFL-LANL. As observed before in laser-ablated films, the large

negative magnetoresistance of the samples screened the Hall signal at temperatures too close to T_c . Unfortunately, our attempts to improve the experimental conditions by increasing the temperature far away from T_c ($T = 500\text{K} \approx 2T_c$), which had been successful in measuring ablated films,³ caused further problems in our present experimental setup. A very large transverse voltage drift (several millivolts over a period of several hours) obscured the Hall voltage at high temperatures. A few conclusions were, nevertheless, extracted.

It was possible to verify that the source of the drift was not electronic, nor did it originate in a temperature change of the sample holder. It was also possible to corroborate that the voltage drift was independent of the rate of change of the magnetic field in the superconducting magnet, discarding thus effects of eddy currents. In addition, we proved that the magnetic history of the sample had no role since we measured similar voltage drifts before and after field cycling the sample at constant temperature. This behavior is displayed in Figures 1 and 2. We interpret the results of these tests as evidence for composition and/or crystallographic order changes at constant temperature in our samples. Further experiments to verify these hypothesis are underway.

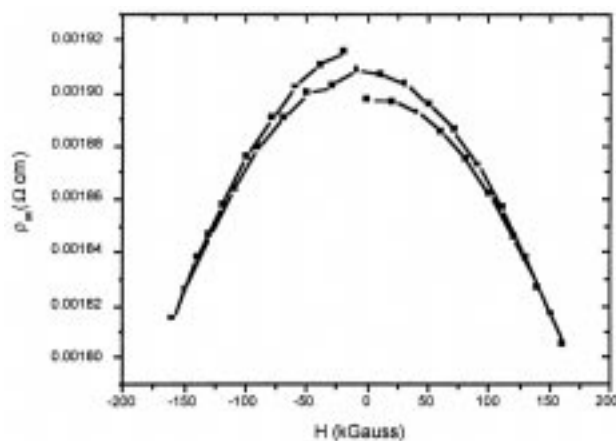


Figure 1. Resistivity of sample 1442-(1,3) at $T = 500$ K vs. magnetic field.

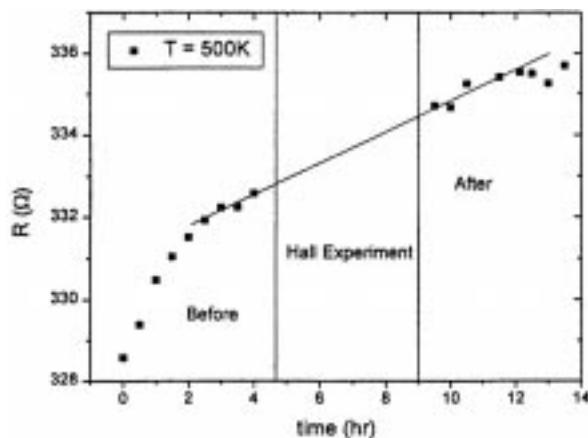


Figure 2. Resistance of sample 1442-(1,3) at $T = 500$ K vs. time, measured before and after the experiment of Figure 1.

References:

- 1 Jaime, M., *et al.*, Appl. Phys. Lett., **68**, 1576 (1996); Jaime, M., *et al.*, Phys. Rev. B, **54**, 11914 (1996).
- 2 Roder, H., *et al.*, Current Opinion in Solid State & Materials Science, **2**, 244 (1997).
- 3 Jaime, M. *et al.*, Phys. Rev. Lett., **78**, 951 (1997).

High Field ESR Study of TDAE-C₆₀ Powder at Different Larmor Frequencies

Maniero, A.L., Univ. of Padova, Italy, Chemistry
Pasimeni, L., Univ. of Padova, Italy, Chemistry
Brunel, L.-C., NHMFL
Cao, G., NHMFL
Pardi, L.A., NHMFL
Guertin, R.P., Tufts Univ., Physics

TDAE (tetrakis-dimethylamino-ethylene)-C₆₀ undergoes a ferromagnetic-like transition at $T_c = 16$ K in freshly prepared samples as measured with low field SQUID magnetometry, confirming previous results. Isothermal SQUID magnetometry was also performed up to 7 T. It is significant that the ordered magnetic phase comes about in an organic material, totally devoid of transition metal constituents, and it is one of the highest transition temperatures for such a system. The transition temperature for a more aged sample of TDAE-C₆₀ was only $T_c = 5$ K. ESR spectroscopy was obtained for both materials, the highest field ESR spectra yet obtained for TDAE-C₆₀, in an attempt to determine the type of magnetic ordering, which has never been satisfactorily resolved.

ESR spectra were recorded for $5 < T < 300$ K at frequencies of 110, 180, 280 and 380 GHz. For both samples there was a shift to lower fields of the resonant fields with decreasing temperature beginning around 80 K and continuing through T_c , the downshift being more pronounced for the lower field portion of the spectra. The shift grows to about -20 mT at lowest temperature. These features are not typical of a classic ferromagnet, but suggest short range order effects. The spectra for the aged sample ($T_c = 5$ K) were similar and differed only in details of the lineshape. For the aged sample, two distinct resonant fields, H_y and H_z were resolved. The features of selected 108 GHz spectra of the newly prepared sample for $T < 80$ K, which are typical of a powder spectrum with anisotropic magnetic susceptibility, were simulated

with a model of $S = 1/2$ spins having an anisotropic g factor.

The major features of the downshifts of the spectra suggest the effect of a local spontaneous field, mostly independent of the applied field. The negative field shifts were fit to a theory of Nagata,¹ which is based on one-dimensional short range ordering between inequivalent classical spins. The exchange and dipolar interaction parameters obtained are of the right order of magnitude for typical one-dimensional antiferromagnets supporting short range ordering induced by exchange and dipolar interactions, even though the theory addresses single dimensional systems. The enhanced resolution provided by the high field ESR spectrometer allowed for the first time detailed determination of the temperature dependence of the spectral downshifts and successful analysis of the results supports short range order even above T_c in TDAE-C₆₀.

References:

- 1 Nagata, K.J., Phys. Soc. Japan, **40**, 1209 (1976).

Local Enhancement of Antiferromagnetic Correlations by Nonmagnetic Impurities

Martins, G., NHMFL
Laukamp, M., NHMFL
Riera, J., Rosario Univ., Argentina, Physics
Dagotto, E., FSU, Physics/NHMFL

The local enhancement of antiferromagnetic correlations near vacancies observed in a variety of spin systems is analyzed in a single framework. Variational calculations suggest that the Resonance-Valence-Bond (RVB) character of the spin correlations at short distances is responsible for the enhancement. Numerical results for uniform spin chains, with and without frustration, dimerized chains, ladders, and two dimensional clusters are in agreement with our conjecture. This short distance phenomenon occurs independently of the

long distance behavior of the spin correlations in the undoped system. Experimental predictions for a variety of compounds are briefly discussed.¹

References:

- ¹ Martins, G., *et al.*, Phys. Rev. Lett., **78**, 3563 (1997).

Pulsed Field Study of the Metal-Insulator Transition in $\text{Ca}_3\text{Ru}_2\text{O}_7$ Using Resistivity and Magnetization

McCall, S., NHMFL
Guertin, R.P., Tufts Univ., Physics
Cao, G., NHMFL
Crow, J.E., NHMFL
Harrison, N., NHMFL/LANL
Mielke, C.H., NHMFL/LANL
Lacerda, A.H., NHMFL/LANL

As reported earlier¹ single crystal $\text{Ca}_3\text{Ru}_2\text{O}_7$, like very few other transition metal oxides, undergoes a metal-to-insulator transition as temperature is lowered through 48 K. We have investigated the field dependence of this transition, which is associated with a nearby antiferromagnetic ordering (Neel) transition at $T_N = 56$ K. The “easy” axis for magnetization is $H \parallel [110]$ in the Ru-O (ab) planes of this bilayered structure. The “hard” axis for magnetization is along the [001] (c-axis). For $H \parallel [110]$ the critical field for reorientation of the spins and concomitant retransition from insulator to metal is only 6 T. We attempted to determine the critical field for the “hard” axis in the 30 T DC magnets of the NHMFL, but could find no such transition to 30 T. The purpose of this search was not only to find the transition, but to determine whether both magnetization and electrical resistivity showed anomalies at the same field, as this would determine if the spin and charge systems were coupled. Utilizing the 50 and 60 T pulsed magnets available at the NHMFL/LANL facility, we were able to determine that the critical field required to induce a metamagnetic transition along the hard [001] axis is 37 T. This indicates that the free energy required to

rotate the spins into the least favorable direction is huge. Furthermore, a drop in the resistivity was also observed at 37 T, which implies that the conduction electrons and magnetic structure are closely correlated. While other layered ruthenate systems have shown charge/spin coupling,² this is the first occurrence to be found under such large applied fields. The very large anisotropy in the magnetic properties of this compound is quite remarkable, and warrants considerable further study.

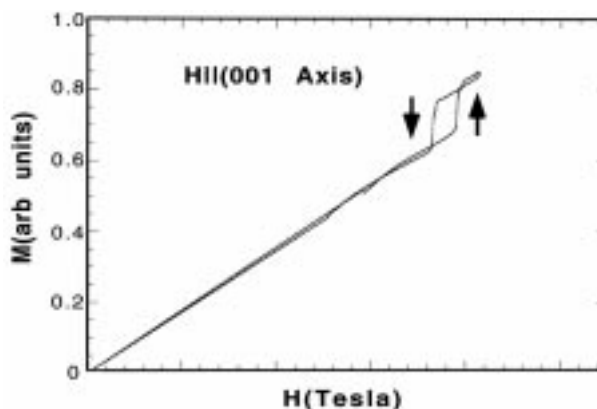


Figure 1. Low temperature magnetization measured along the “hard” [001] axis.

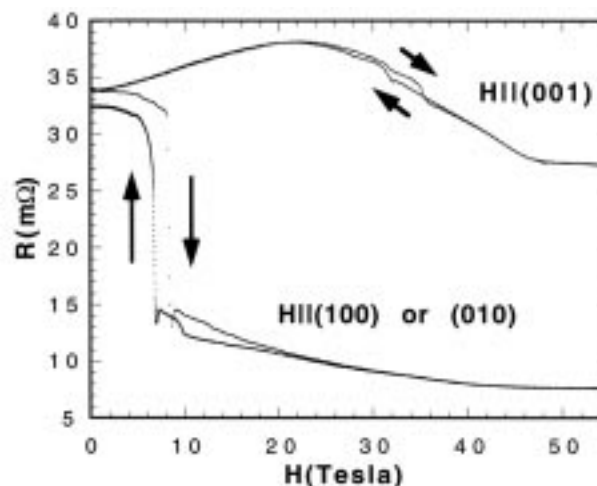


Figure 2. Low temperature magnetoresistivity measured along [010] or [100], close to the “easy” [110] axis, and along the “hard” [001] axis. Both measurements show a non-metal to metal transition at $H_c = 37 \pm 1$ T along the hard axis.

References:

- ¹ Cao, G., *et al.*, Phys. Rev. Lett., **78**, 1751 (1997).
² For example: Cao, G., *et al.*, Phys. Rev. B, **56**, 321 (1997).

High Field EPR of the Dilute Magnetic Semiconductors Cd(.55)Mn(.45)Se and Cd(.7)Mn(.3)Se

McCarty, A., NHMFL/FSU, Physics
Hassan, A.K., NHMFL/FSU, Physics
Martins, G. B., NHMFL
Furdyna, J.K., Univ. of Notre Dame, Physics
Brunel, L.-C., NHMFL

To understand the interactions in magnetic systems like dilute magnetic semiconductors (DMS), it is of interest to determine the field and frequency dependence of the Dzyaloshinski-Moriya (DM) interactions in these semiconductors. The DM interaction is the anisotropic part of the Mn-Mn interactions. Larson and Ehrenreich conjectured that EPR spectroscopy offers the best opportunity to determine the anisotropic superexchange in DMS because the anisotropic exchange significantly broadens the line by suppressing exchange narrowing.¹ At low temperature, the linewidth is more narrow at high fields, in the regime where the Zeeman energy exceeds the anisotropic exchange energy, than it is for low fields. At low fields, the ions are coupled; while at high fields, they act independently.

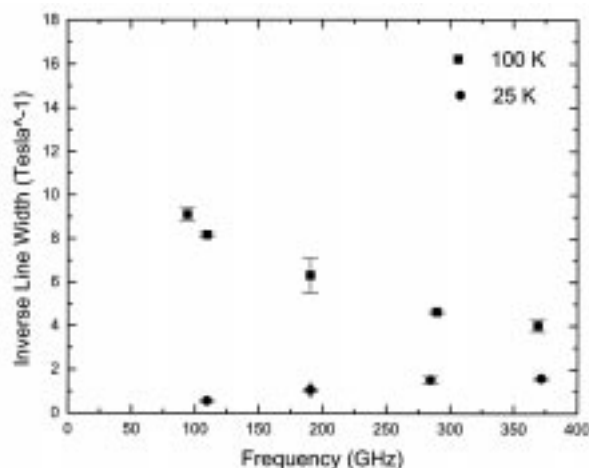


Figure 1. Inverse linewidth vs. frequency for Cd(.55)Mn(.45)Se.

Also, we observe a shift in the resonance position with decreasing temperature. We conclude that this shift in resonance position is due to an internal field. This internal field is dependent on temperature and on Mn concentration. The magnitude of the internal field is determined by the intercept of a plot of experimental resonance position versus frequency. This work was performed at the frequencies of 95, 110, 190, 285, 380 GHz.

References:

- ¹ Larson, B.E., *et al.*, Phys. Rev. B, **39**, 1747 (1989).

Glassy Behavior in the Random-Field System Fe_{0.60}Zn_{0.40}F₂ at Intense Fields

Montenegro, F.C., UFPE-Brazil, Physics
Lima, K.A., UFPE-Brazil, Physics
Torikachvili, M.S., San Diego State Univ., Physics
Lacerda, A.H., NHMFL/ LANL

Most the experimental work in the dilute antiferromagnetic (DAF) compound Fe_xZn_{1-x}F₂, in the context of the random-field Ising model (RFIM), has been performed under relatively low magnetic fields (H) applied along the easy axis. In this work the critical and irreversibility phase boundaries of the d = 3 dilute uniaxial antiferromagnet Fe_{0.60}Zn_{0.40}F₂ have been determined under strong magnetic fields via magnetization measurements performed at the NHMFL-LANL. The data reveal that the random-field-induced glassy phase, previously reported¹ in the upper part of the (H, T) phase diagram for highly diluted samples (Fe concentration x = 0.3), is extended to higher values of x.

The phase diagram found shows that the critical boundary T_c(H) departs from the standard random-exchange to the RFIM crossover scaling (i.e., T_N - bH² - T_c(H) = CH^{2/φ}, with φ ~ 1.4) for H > 5 T. The upper equilibrium boundary H_{eq}^μ(T), changes from a concave to a convex shape, delimiting the onset of the glassy phase. A new

irreversibility line, $H_{eq}^l(T)$, has been discovered in this experiments. Below $H_{eq}^l(T)$, the anti-ferromagnetic configuration is recovered when the field is decreased from the paramagnetic phase.

References:

- 1 Montenegro, F.C., *et al.*, Phys. Rev. B, **44**, 2155 (1991); *ibid* p. 2161.

Spectroscopic Studies of Spin-Peierls Materials in a Magnetic Field

Musfeldt, J.L., State Univ. of New York (SUNY)-Binghamton, Chemistry
Wang, Y.J., NHMFL
Li, G., SUNY-Binghamton
Long, V.C., SUNY-Binghamton

The prototypical spin-Peierls materials GeCuO_3 and $\text{MEM}(\text{TCNQ})_2$ have attracted a great deal of interest recently.^{1,2} In both cases, interest has focused on the magnetic-field/temperature phase diagram, which has three characteristic phases. In order to investigate the nature of the spin-Peierls transition and behavior of the uniform, dimerized and magnetic phases, we have made infrared transmission measurements of $\text{MEM}(\text{TCNQ})_2$ and the optical reflectance measurements of GeCuO_3 as a function of temperature and applied magnetic field. Our goal is to characterize the microscopic nature of these competing broken symmetry ground states.

Our first set of experiments explored the optical spectra of GeCuO_3 , the prototypical inorganic spin-Peierls material. Typical data is shown in Figure 1.

We are analyzing the 1.47 eV feature within two different pictures, either as a pull-back of the band edge or as an exciton of the phonon-assisted red-band.³ The energy of this structure is consistent with the first possibility, whereas the pronounced vibrational fine structure within the envelope is in

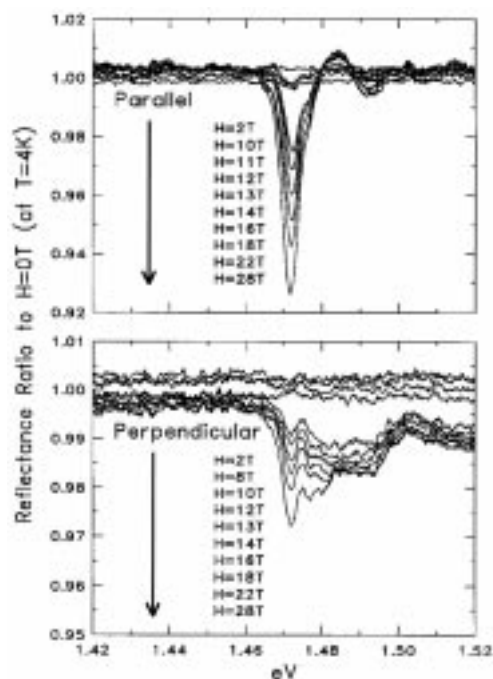


Figure 1. Ratio of reflectance at high magnetic field to the zero field reflectance for polarization parallel to the c-axis (upper panel) and perpendicular to the c-axis (lower panel), all at 4 K.

line with the second theory. We are currently working to distinguish between these two possibilities. Further, we are pursuing the relationship between the 1.47 eV structure and the order parameter (and the opening of the magnetic gap) of the dimerized phase.

Our second set of experiments explored the far-infrared magneto-elastic coupling in $\text{MEM}(\text{TCNQ})_2$, a traditional organic molecular conductor, as a function of temperature and magnetic field. The measurements carried out in a magnetic field allowed us to probe the nature of the high-field phase and the driving forces of the spin-Peierls \rightarrow magnetic phase transition. Within our noise level (3%), we find that the electron-phonon coupling-induced modes and the low-energy lattice modes do not display any changes on passing through the high-field phase boundary. This shows that the activated A_g modes are most sensitive to changes in the conduction electrons, rather than to the magnetic microstructure of the high-field phase. This is in contrast to the new inorganic spin-Peierls material, GeCuO_3 , which has both a stiffer lattice, a more localized spin

structure, and significant two-dimensional magnetic interactions.

References:

- ¹ Hase, M., *et al.*, Phys. Rev. Lett., **70**, 3651 (1994).
- ² Bray, J., *et al.*, in *Extended Linear Chain Compounds*, edited by J.S. Miller (Plenum, New York, 1983), Vol. 3.
- ³ Perkins, J.D., *et al.*, Phys. Rev. Lett. **71**, 1621 (1993).

Magnetic Transitions in UNiGe

Nakotte, H., New Mexico State Univ. at Las Cruces, Physics
Lacerda, A.H., NHMFL/LANL
Torikachvili, M.S., San Diego State Univ., Physics
Prokes, K., Hiroshima Univ., Japan, Physics

In zero field, UNiGe undergoes two magnetic transitions at about 50 K and 42 K, and both magnetic structures have been identified previously by neutron diffraction.¹ Here, we performed temperature scans of the magnetization in static magnetic fields up to 19.5 T using the 20 T superconducting magnet at the NHMFL Pulsed Field Facility at Los Alamos. For fields applied along the b and c-axes, we observe clear anomalies in the magnetic response, which occur at the magnetic transitions. We confirmed the previously reported phase boundaries in the B-T diagram for field applied along the c-axis,¹ and in addition we determined the location of the phase boundaries for field applied along the b-axis. Apart from the two low-field phases, for both orientations a third magnetic phase occurs in higher applied fields (at 4 K: >3 T for B//c and >18 T for B//b). Our magnetization results are consistent with a relationship between the three magnetic phases, which has been proposed earlier.¹ In addition, we find evidence for complex domain effects to occur in UNiGe close to the magnetic phase boundaries.

References:

- ¹ Nakotte, H., *et al.*, Phys. Rev. B, **54**, 7201 (1996).

Magnetization Measurements of Colossal Magnetoresistance Oxides

Neumeier, J.J., Florida Atlantic Univ., Physics
Goodwin, D.H., Florida Atlantic Univ., Physics
Torikachvili, M.S., San Diego State Univ., Physics
Lacerda, A.H., NHMFL/LANL

An enormous amount of effort is presently being concentrated on the study of an exceptionally large magnetoresistance in manganese oxides. The magnetoresistance is commonly larger than 90% and is referred to as colossal magnetoresistance or CMR.¹ CMR results from a strong interplay amongst magnetic, structural, and electrical transport properties.^{1,2} Theoretical³ and experimental results^{1,2} point to the existence of lattice distortions, or polarons, which possess both charge and magnetic character. The magnetic polarons delocalize below the ferromagnetic transition temperature T_c , thus permitting formation of a metallic state.

Characterization of the magnetic polarons will reveal their size, i.e. how many lattice sites on average each polaron encompasses, and the influence of temperature on their formation. We are attempting to obtain this information by measuring the magnetization M as a function of field above T_c in the paramagnetic state. In the CMR oxides, two neighboring magnetic ions are magnetically coupled via the process of an electron hopping from one ion to the next, this is called double exchange.³ The magnetic moments that result in the paramagnetic M will consist of two species. The first is uncoupled moments, the second is composed of two or more moments that point in the same direction (these are coupled by double exchange). The moments coupled by double exchange result in an enhancement of M . This is illustrated in Figure 1 where we show M as a function of magnetic field for two temperatures above T_c . These data were measured with the 20 T vibrating sample magnetometer at NHMFL-Los

Alamos. Note that there is no saturation at low field, which would indicate the existence of ferromagnetic domains. This illustrates that M is indeed "paramagnetic-like." For comparison, we have plotted M in the Curie-Weiss limit as the dashed line; there is clearly a significant enhancement of M in the low-field limit. At the highest fields, M reaches over 50% of the ferromagnetic saturation moment observed at 5 K ($M(5\text{ K}) = 3.71\ \mu_B/\text{Mn-ion}$). We are developing a simple theoretical description of the data based on statistical arguments and electrical transport data.

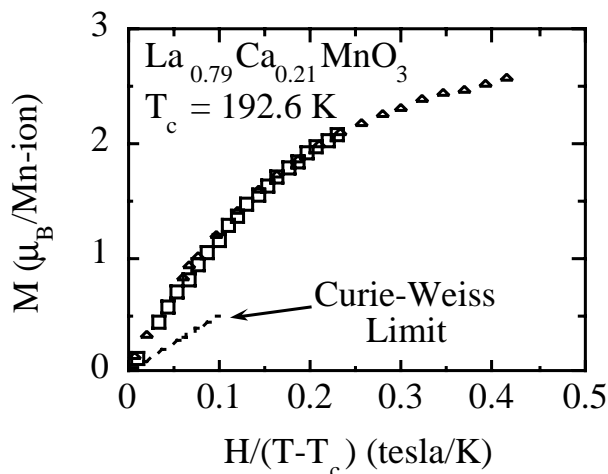


Figure 1. Magnetization vs. $H/(T-T_c)$ at 235 K (diamonds) and 270 K (squares). The dashed line is the magnetization expected in the Curie-Weiss limit.

References:

- 1 Hundley, M.F., *et al.*, Appl. Phys. Lett., **67**, 860 (1995); and ref. therein.
- 2 Booth, C.H., *et al.*, to be published in Phys. Rev. Lett. **80** (1998); and ref. therein.
- 3 Millis, A.J., *et al.*, Phys. Rev. Lett., **77**, 5144 (1996).

High Field Magnetic Properties of a New Class of Nd-Fe-Al Based Hard Magnetic Bulk Amorphous Alloy

Ortega, R., Dept. de Física, Universidad Pública de Navarra, Pamplona, Spain

Rao, K.V., Condensed Matter Physics, Royal Institute of Technology, Stockholm, Sweden

Inoue, A., Inst. of Materials Research, Tohoku University, Sendai, Japan

Project Goals. Recently a new class of amorphous materials in the form of rods of diameter 3 to 10 mm have been fabricated at rather low quenching rates than known possible hitherto. This project is to investigate the high field magnetic properties of bulk amorphous hard magnets in fields up to 30 T over the temperature range 1.25 K to room temperature. This work is motivated by the experimental fact that these hard amorphous magnets do not saturate in fields below 5 T, and that the temperature dependence of the coercivity exhibits an unusual maximum at around 70 K. The maximum value of coercivity around 2.7 T determined in a maximum external field of 5 T is itself perhaps the highest value observed for the coercivity of any hard magnet. It is thus of interest to investigate the magnetic properties of these novel materials at higher fields to understand the basis for such unusual properties of these new class of hard magnets.

Introduction. Amorphization of metals has been known for almost four decades, ever since the first preparation of a man-made glassy metallic alloy by Paul Duwez and his coworkers.¹ Our comprehension hitherto of the amorphization of metallic alloys has been radically challenged by the recent significant developments in this field. From a conventional understanding that quenching rates around 10^6 K/s are essential in order to produce a metallic amorphous alloy, which is by necessity of the order of few microns

thin at least along one of its dimensions, the new class of amorphous materials are *bulk* and cooled from the liquid state at a rate even much lower than that for obtaining the silica glass of our windows! The observed large glass forming ability of these multicomponent metallic alloys has been ascribed to their large negative heat of mixing and different atomic size ratios.² Indeed the fabrication of a glassy metallic Nd₆₀Fe₃₀Al₁₀ in the form of a rod 3–6 mm in diameter requires cooling rates lower than 1 K/s. The material is found to be an isotropic hard magnet with coercivities above 4 kOe, at room temperature, in applied fields of 50 kOe. Surprisingly, rapid quenching of the same ingot is found to produce a nanocrystalline, soft magnet at room temperature.

Microstructural characterization of the bulk material using optical microscopy, X-ray diffraction, SEM, TEM, did not show any crystalline phase in the as cast state. From an analysis of the radial distribution function from X-ray diffraction, clusters of Fe were evidenced, i.e., regions where the coordination number of Fe around Fe was found to be larger than for the random alloy. The hard magnetic properties were found to irreversibly degrade upon annealing above 650 K, crystallizing at 784 K into hcp Nd, cubic Al₂Nd and tetragonal δ -Nd₃Fe_{1-x}Al_x, with no indication of a glass transition temperature.³

Experiments at the NHMFL. A set of experiments was carried out at the NHMFL facilities: starting from the thermally demagnetized state, loops cycled at increasingly higher magnetic fields were measured at temperatures in the range 1.2 K to room temperature, of which the ones at 1.2 and 30 K, cycled at 20 T and 15 T respectively, are shown in Figure 1. Fields larger than 15 T were required to close the loops, which did not saturate at fields even as large as 30 T. A maximum in the intrinsic coercivity, shown at the inset, was observed around 30 K. Nevertheless, by realizing that the differential susceptibility of the major loop at 1.2 K was closing at fields close to 6 T, and that

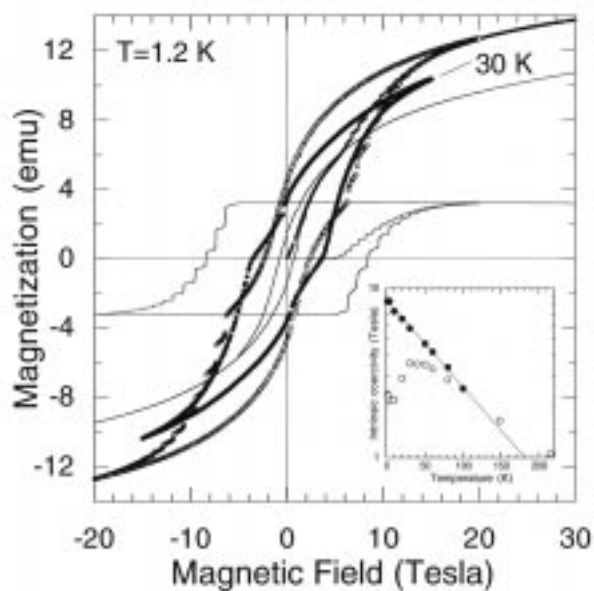


Figure 1. Experimental hysteresis loop and virgin curve at 1.2 K (open circles) and at 30 K (closed circles); the superposition of the two deconvoluted loops (solid lines) gives the experimental one. *Inset:* temperature dependence of the intrinsic coercivity from the experimental hysteresis loop (○), and from the deconvoluted hard loop (●). The solid line is a fit to the expression $H_c(T) = H_c(0)e^{-\Delta/T}$, where $\Delta = 85$ K and $\mu_0 H_c(0) = 8.47$ T. (Sample mass: 149 mg).

the loops became sigmoidal below 60 K, thus suggesting the existence of two distinct magnetic phases, the loop at 1.2 K was deconvoluted into the two ones shown by solid lines. The *hard*, almost square hysteresis loop, has been ascribed to the magnetization of the clusters of ferromagnetically coupled Fe spins, which in turn seemed to be antiferromagnetically coupled to the neighboring Nd spins. The *soft* one may be ascribed to the Nd-rich amorphous matrix, with a net antiferromagnetic interaction. The intrinsic coercivity of the *hard* loop exhibits an exponential temperature dependence of the intrinsic coercivity, also shown at the inset. Such dependence had been observed in melt-spun ribbons of Fe with Nd, Pr or Sm, and attributed to the formation of a fine microstructure of metastable quasicrystalline or glassy phases.⁴ The observed anomalous temperature dependence of the coercivity is, in this case, attributable to the different temperature dependencies of the magnetization of each

phase. At higher temperatures, above 100 K, the antiferromagnetic-like component of the overall magnetization drops, and hence the intrinsic coercivity is mainly due to the ferromagnetic phase.

Efforts are in progress to fabricate an isotropic, bulk glassy magnet consisting of only the hard phase observed in the material described above. As is now, its remanence would exceed 1.3 T and its maximum energy product would be 360 kJ/m³, at 1.2 K. Preliminary magnetic measurements to understand the well defined steps observed in the hysteretic loops at 1.2 K, at external fields above 5 T, show that the steps are observed only below 4 K and is related to some new intrinsic phenomenon involving exchange coupling among the rare-earth rich and F-rich regions in these glassy bulk materials. Further studies on this property are in progress.

Acknowledgements. This work could not have been realized without the careful, invaluable help of Christian Wolters, from the NHMFL. Discussions during the course of the measurements with J. Crow and B. Guertin are greatly appreciated.

References:

- ¹ Klement, W., Jr., *et al.*, *Nature*, **187**, 869 (1960).
- ² Inoue, A., *et al.*, *Mater. Trans. JIM*, **30**, 965 (1989); *J. Non-Cryst. Solids*, **156-158**, 473 (1993); *Materials Sci. Forum*, **179-181**, 691 (1995); *Mater. Trans. JIM*, **36**, 866 (1995); *Nanostructured and Non-Crystalline Materials*, eds. by M. Vázquez, *et al.*, p. 15 (World Scientific, Singapore, 1995); *Mater. Trans. JIM*, **37**, 99 (1996).
- ³ Matsubara, E., *et al.*, *Sci. Rep. RITU*, **A43**, 83 (1997); Inoue, A., *et al.*, *Mater. Trans. JIM*, **37**, 99 (1996).
- ⁴ Moorjani, K., *et al.*, *Coey. Magnetic Glasses*, p 284, and ref. cited therein (Elsevier, Amsterdam, 1984).

High Field EPR of One-Dimensional Heisenberg System of Formula $\text{Ni}_x\text{Zn}_{1-x}(\text{ox})\text{L}_2$

Pardi, L., NHMFL

Redijk, J., Univ. of Nijmegen, The Netherlands

Hulsbergen, F.U., Univ. of Nijmegen, The Netherlands

Brunel, L.-C., NHMFL

The direct measurement of the sign and magnitude of the zero field splitting of $\text{Ni}_x\text{Zn}_{1-x}(\text{ox})\text{L}_2$ (where ox = oxalate and L is an imidazole) in the low Nickel concentration range ($x = 0.07, 0.10$) using high field EPR spectroscopy was the subject of last year's report. The study was aimed at the determining the zero field splitting parameters in a Haldane system. That experiment turn out to be a school case in the study of orientation effects of powdered samples, in the light of which other experiments in high field could be interpreted easily.

Pursuing the investigation of this series of compounds in order to determine the onset of Haldane behavior as a function of x , we measured the EPR spectra of $\text{Ni}_x\text{Zn}_{1-x}(\text{ox})\text{L}_2$ for x values ranging from 0.13 to 0.50. Several frequencies were used in the range from 95 GHz to 440 GHz.

All the samples show half field transitions (HFT), that is, transitions that fall at values of field which are about half of the value expected for the $g = 2$. These signals are associated with an extended fine structure (FS) at Ni concentrations of 0.2 ca. For high Ni concentration ($x = 0.43$ and 0.49), a new signal is observed at $g = 2.2$ whose intensity goes through a maximum at 30 K ca. The HFT and the associated FS are attributed to isolated Nickel ions or small Nickel clusters with an $S = 1$ ground state. The $g = 2.2$ signal is from an excited state and could be the fingerprint of Haldane behavior.

Investigation of Low-Dimensional Magnetic Materials by High Field EPR Spectroscopy

Pardi, L., NHMFL

Gatteschi, D., Univ. of Florence, Italy

Caneschi, A., Univ. of Florence, Italy

Brunel, L.-C., NHMFL

EPR spectroscopy is well known to be a valuable tool in assessing the magnetic dimension of materials. Systems in which exchange coupling is operative along one or two crystallographic directions are generally termed "low-dimensional magnetic materials." The EPR spectra of these systems show a peculiar behavior that is determined by the fact that exchange narrowing operative in one or two dimensions is less effective than in three-dimensional systems. In the high temperature limit ($kT \gg J$) that is in the ideal paramagnetic phase, the EPR lineshape and linewidth depend upon the orientation of the crystal with respect to the magnetic field. In one-dimensional systems this gives rise to the so called magic angle behavior for which a minimum of the linewidth is observed when the field makes an angle of 54° with respect to the direction of the chain. As the temperature is lowered, and the system still in the paramagnetic phase, short range order effects become operative. These effects are observed as g-shifts whose sign and size depend on the nature and magnitude of the exchange coupling and the interplay of exchange and dipolar interactions.

A series of linear chain complexes made of Gd(III) ions bridged by nitronyl-nitroxide organic radicals were investigated by High Field EPR spectroscopy. Marked g-shifts were observed in the powder spectra of these materials as a function of temperature. The systems also show an interesting splitting of the signals at temperature below 4 K which can be attributed either to a structural or to a magnetic phase transition.

Magnetization and Its Relaxation in Mn_{12} -Acetate

Perenboom, J.A.A.J., KUN-HFML, Nijmegen, The Netherlands, Physics

Brooks, J.S., FSU, Physics/NHMFL

Hill, S.O., FSU, Physics/NHMFL

Dalal, N.S., FSU, Chemistry/NHMFL

Hathaway, T., FSU, Chemistry/NHMFL

We have studied the magnetization (and its relaxation) of single crystals of the Mn_{12} cluster complex $[\text{Mn}_{12}\text{O}_{12}(\text{CH}_3\text{COO})_{16}(\text{H}_2\text{O})_4] \cdot 2\text{CH}_3\text{COOH} \cdot 4\text{H}_2\text{O}$ with the very sensitive cantilever magnetometer in the temperature range from 3 K down to 60 mK. At cryogenic temperatures the cluster behaves as a single $S=10$ object.^{1,2} Below the blocking temperature of about 3 K, the magnetic moment induced by a magnetic field becomes frozen and when the magnetic field is removed or reversed it will only slowly relax with a relaxation time that may exceed 10^8 s. The Mn_{12} -cluster is believed to exhibit macroscopic quantum tunneling of magnetic moment across the barrier between the wells produced by the strong uniaxial anisotropy in the crystal. This is evidenced by steps in the magnetization when magnetic energy levels in the two wells are lined up: we have observed resonances indexed from $N=1$ to

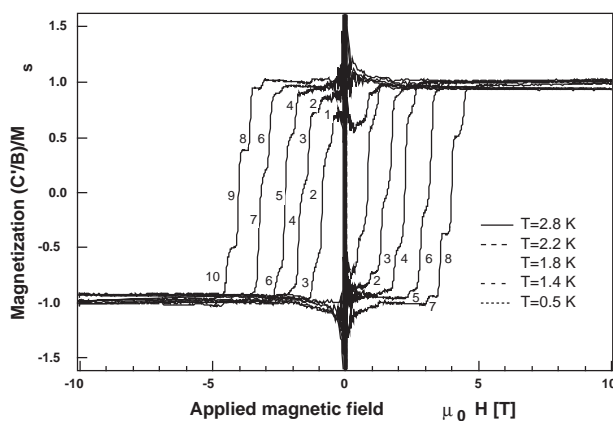


Figure 1. Magnetization of a Mn_{12} -acetate single crystal with the magnetic field aligned along the easy axis and for several different temperatures. The sample is first fully magnetized, and rapid changes in the magnetization occur at resonance fields regularly spaced with interval $\Delta B=0.45$ T after the magnetic field has been reversed.

$N=11$ (at temperatures well below 1000 mK), see Figure 1. The hysteresis in the magnetization observed for different ramping rates of the magnetic field and for different temperatures below the blocking temperature points to the energy barrier that exists to slow down the relaxation. It was found that the relaxation rate at a step in the magnetization curve is almost an order of magnitude stronger for each higher index transition and temperature dependent down to at least 500 mK. Our measurements also show that at low temperatures the relaxation near a step in the magnetization curve is logarithmic with time (indicating that there are several different barriers for the relaxation of the magnetization remaining after a resonant step).

Analysis of the cluster using an effective spin Hamiltonian suggested the presence of significant fourth-order anisotropy and subsequent microwave-frequency spectroscopic studies have brilliantly confirmed the parameters used in this approach, allowing us to resolve the disagreement between the values for the height of the energy barrier derived in the literature from magnetization and thermal relaxation on the one hand and high-energy EPR on the other.

Our understanding of the relaxation process is now that when the system is brought to resonance by increasing the magnetic field to near a step a thermal avalanche of phonons produced when some clusters relax to the ground state ($m=+10$) produces a non-thermal distribution over the available excited levels in the well separated by an anisotropy barrier from the ground state (i.e. antiparallel spin orientations) facilitating subsequent relaxation of some of the excited populations through tunneling across the barrier. The fourth-order anisotropy and accidental misalignment between applied magnetic field and the easy axis of the crystal then provide the coupling necessary for realigning the spin of the cluster. Our data did not allow yet to identify which specific levels are most effective for the tunneling process.

References:

- ¹ Friedman, J.R., *et al.*, Phys. Rev. Lett., **76**, 3830 (1996).
- ² Thomas L., *et al.*, Nature, **383**, 145 (1996).

Phase Diagram of Electronic Models for Transition Metal Oxides in One Dimension

Riera, J., Rosario Univ., Argentina, Physics
Hallberg, K., Centro Atomico, Bariloche, Argentina
Dagotto, E., FSU, Physics/NHMFL

The zero temperature phase diagram of the ferromagnetic Kondo model in one dimension is studied using numerical techniques, specially at large Hund coupling. A robust region of fully saturated ferromagnetism (FM) is identified at all densities. Phase separation between hole-rich and hole-poor regions and a paramagnetic regime with quasi-localized holes were also observed. It is argued that these phases will also appear in two and three dimensions. As the transition metal ion spin grows, the hole mobility rapidly decreases explaining the differences between Cu-oxides and Mn-oxides.¹

References:

- ¹ Riera, J., *et al.*, Phys. Rev. Lett., **79**, 713 (1997).

Thermal Transport in $\text{Sr}_{1-x}\text{Ca}_x\text{RuO}_3$

Shepard, M., NHMFL
Henning, P.F.,* NHMFL
Cao, G., NHMFL
Crow, J.E., NHMFL

We have studied the thermal conductivity $K(T, B)$ ($6 < T < 250$ K, $0 < B < 15$ T) of single crystals of SrRuO_3 , a ferromagnet with $T_c = 160$ K, and isostructural but paramagnetic CaRuO_3 , as well as the intermediate crystals $(\text{Sr,Ca})\text{RuO}_3$ for the purpose of probing charge carrier (K_e), phonon (K_p), and magnon (K_m) excitations in these systems. The contributions of electron and phonon scattering processes to the thermal conductivities have been estimated using a Wiedemann-Franz relationship to estimate K_e thus obtaining K_p at

higher temperatures. Roughly 50% of the thermal conductivity is estimated to be phononic near room temperature. Amorphous behavior is observed in the doped samples, and no break in the thermal conductivity is seen at the ferromagnetic onset. A comparison of magnetothermal conductivity and magnetoresistivity measurements at lower temperatures in SrRuO_3 and CaRuO_3 reveals that additional scattering mechanisms have become important. These investigations argue for the importance of phonon and magnon contributions, in addition to electronic contributions, to the magnetic behavior in $\text{Sr}_{1-x}\text{Ca}_x\text{RuO}_3$ systems.

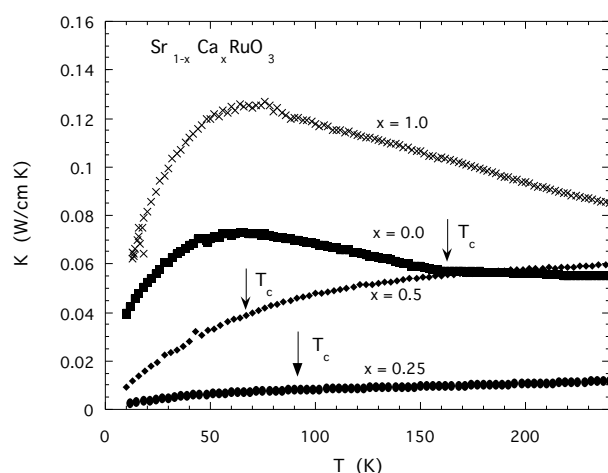


Figure 1. Thermal conductivity as a function of temperature for $x=0, 0.25, 0.50$, and 1.0 .

* Present address: Brookhaven National Laboratory, Physics Dept., Upton, NY.

Miniature Magnetoresistance Probe for High-Field Measurement

Xia, J.S., NHMFL/UF, Physics
Sullivan, N.S., NHMFL/UF, Physics
Adams, E.D., NHMFL/UF, Physics

A miniature magnetoresistance (MR) probe has been designed and tested in conjunction with ^3He NMR to determine the field-current ratio B/I , homogeneity, field profile, and persistence of the 8 T and 17 T superconducting magnets of the NHMFL High B/T Facility.

The MR probe, 1 mm diameter x 2.5 mm long, was wound bifilarly on an epoxy former using a 40-m length of 25 μm diameter pure copper wire. The four-terminal resistance, measured with an HP 3457A multimeter, was 235 Ω at room temperature, decreasing to 2.866 Ω at 4.2 K in zero applied field. The probe was mounted with its axis perpendicular to the field axis.

The two-magnet system tested with this probe consists of an 8 T magnet for adiabatic demagnetization and a 17 T magnet for measurements of the field-dependence of various properties. The 17 T magnet has a homogeneity of better than 2×10^{-5} over 1-cm-diameter volume, sufficient for moderate-resolution NMR. A 493-MHz ^3He NMR probe was used to determine the field of the magnet at 15.20 T and from this the ratio of field-to-current B/I for the magnet.

Then, the MR probe was centered in the field and calibrated by operating the magnet at various currents, with the results shown in Figure 1. At low fields, the sensitivity dR/dB is low; however, it rises rapidly with field to 0.5 Ω/T above about 4 T, where it becomes almost constant. Resolution in resistance of 10^{-4} Ω corresponds to a field resolution of 3×10^{-5} T. Reproducibility on thermal cycling to room temperature and back several times was 2×10^{-3} Ω at 15 T.

The calibrated probe, mounted on the end of a long stainless steel tube extending through a sliding seal in the top-plate of the dewar, was moved along the axis of the two-magnet system to determine the field profile. The position of the probe was determined from the length of the support tube extending outside the dewar.

Near the center of the 17 T magnet, the field was measured by both the MR and NMR probes, with differences between the two determined by the uncertainty in positions of the probes. Measurement of the field away from the center with the NMR probe is not possible because of the reduced homogeneity, even if a variable-frequency spectrometer were available. The decay of the 17

T magnet in the persistence mode was 2×10^{-5} per day, measured by observing changes in the MR probe and the NMR frequency over a 24-hour period.

A small inexpensive copper wire magnetoresistance probe has been shown to be useful for measuring the homogeneity, persistence, and field profile of superconducting magnets.

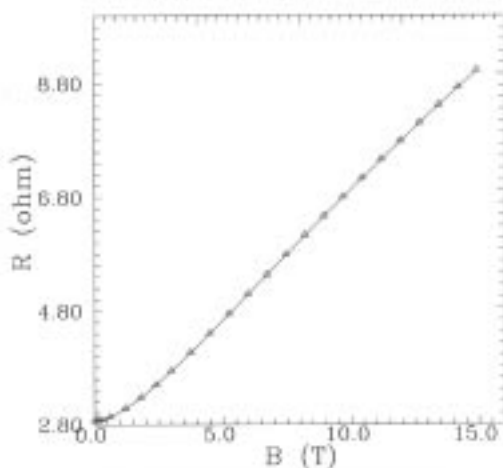


Figure 1. Probe resistance vs. magnetic field.

Magnetic Properties of the 2D Magnetic System $\text{CsFe}_x\text{Ag}_{2-x}\text{Te}_2$

Yuen, T., Temple Univ., Physics

$\text{CsFe}_{0.72}\text{Ag}_{1.28}\text{Te}_2$ is a newly synthesized quasi-ternary telluride compound. Its crystal structure is of a ThCr_2Si_2 type with space group $I4/mmm$, in which the Fe and Ag form a two-dimensional (2D) square network.¹ Results of initial studies² using temperature dependent and field dependent (up to 5.5 T) magnetization, heat capacity, and ^{57}Fe Mössbauer spectroscopy show that $\text{CsFe}_{0.72}\text{Ag}_{1.28}\text{Te}_2$ exhibits two magnetic phase transitions at $T_1 > 400$ K, and $T_2 = 123$ K. The first magnetic transition at T_1 is of a canted antiferromagnetic type. The second transition at T_2 is also of an antiferromagnetic kind with a magnetic moment reorientation. The anomaly seen in the heat capacity confirms the transition at 123 K. The Mössbauer studies reveal large magnetic

splitting at the two Fe sites and the existence of two distinguished ionization states of Fe (Fe^{2+} and Fe^{3+}) in the 2D network.

To further study the nature of the magnetic ordering in $\text{CsFe}_x\text{Ag}_{2-x}\text{Te}_2$, we performed measurements of the temperature dependent magnetization, $M(T)$, and isothermal magnetization, $M(H)$. The experiments were carried out during the period of August 4 to August 12, 1997. A vibration sample magnetometer was used in Cell #9 with a 30 T magnet. We measured $M(T)$ and $M(H)$ on randomly oriented and field aligned polycrystalline samples of $\text{CsFe}_{0.72}\text{Ag}_{1.28}\text{Te}_2$. We also measured the magnetization of the randomly oriented polycrystalline samples of CsFeAgTe_2 . The temperature range of these measurements was from 5 K to room temperature and the field range was from 0 to 30 T.

The above reported studies at NHMFL enriched our knowledge about the magnetic properties of the $\text{CsFe}_x\text{Ag}_{2-x}\text{Te}_2$ system and confirmed our interpretations of the magnetic structures at the different phases. As we expected,³ the $M(H)$ of $\text{CsFe}_{0.72}\text{Ag}_{1.28}\text{Te}_2$ in the ground state ($T < 123$ K) indicates a canted antiferromagnetic structure, namely, the shape of the $M(H)$ looks like that of a ferromagnetic type but with an unsaturated behavior up to 30 T. Also as expected, The $M(H)$ curve for $\text{CsFe}_{0.72}\text{Ag}_{1.28}\text{Te}_2$ shows a clear slope change at $H = 12$ T in the temperature range of 130 K to 300 K. The slope change is due to a field induced magnetic moment reorientation in a different canted antiferromagnetic phase. This slope change is more significant for the field oriented sample than that for the randomly oriented samples. In addition, as we expected, the magnetic transition at 123 K observed in $M(T)$ under a field below 5.5 T disappeared when a 20 T field was applied. This property is consistent with our argument about the nature of the magnetic ordering in this system. We also performed measurement of $M(H)$ on CsFeAgTe_2 . The crystal structure of this compound is the same as $\text{CsFe}_{0.72}\text{Ag}_{1.28}\text{Te}_2$. Our preliminary results show

a similar magnetic behavior as seen in $\text{CsFe}_{0.72}\text{Ag}_{1.28}\text{Te}_2$.

The results of the above discussed study is to be presented in the 1998 APS March Meeting⁴ and a paper is in preparation for submission to Physical Review B with more detailed analysis and interpretation. This project is supported by NSF Grant DMR 9633018.

References:

- ¹ Li, J., *et al.*, Chem. Mater., 7, 599 (1995).
- ² Yuen, T., *et al.*, submitted to J. M.M.M.
- ³ Yuen, T., proposal submitted for this project, June, 1997.
- ⁴ Yuen, T., *et al.*, abstract accepted for 1998 APS March Meeting.

Static and Dynamical Properties of the Ferromagnetic Kondo Model with Direct Antiferromagnetic Coupling Between the t_{2g} Localized Electrons

Yunoki, S., NHMFL

Moreo, A., NHMFL/FSU, Physics and MARTECH

The phase diagram of the Kondo lattice Hamiltonian with ferromagnetic Hund's coupling in the limit where the spin of the localized t_{2g} electrons is classical is analyzed in one dimension as a function of temperature, electronic density, and a direct antiferromagnetic coupling J' between the localized spins. Studying static and dynamical properties, a behavior that qualitatively resembles experimental results for manganites occurs for J'/t smaller than 0.11. In particular a coexistence of ferromagnetic and antiferromagnetic excitations is observed at low-hole density in agreement with neutron scattering experiments on $\text{La}_{2-2x}\text{Sr}_{1+2x}\text{Mn}_2\text{O}_7$ with $x = 0.4$. This effect is caused by the recently reported tendency to phase separation between hole-rich ferromagnetic and

hole-undoped antiferromagnetic domains in electronic models for manganites. As J' increases metal-insulator transitions are detected by monitoring the optical conductivity and the density of states. The magnetic correlations reveal the existence of spiral phases without long-range order but with fairly large correlation lengths. Indications of charge ordering effects appear in the analysis of charge correlations.

Optical Study of Antiferromagnetic Single-Crystals $\text{Y}_{1-x}\text{Pr}_x\text{Ba}_2\text{Cu}_3\text{O}_6$ in High Magnetic Fields

Zibold, A., UF, Physics

Liu, H.L., UF, Physics

Tanner, D.B., UF, Physics/NHMFL

Wang, J.Y., NHMFL

Grüninger, M., Universität Karlsruhe, Physics

Geserich, H.P., Universität Karlsruhe, Physics

Kopp, T., Institut für Theorie der kondensierten Materie, Universität Karlsruhe

Wolf, Th., Forschungszentrum Karlsruhe

Widder, W., Universität Bayreuth, Physics

Braun, H.F., Universität Bayreuth, Physics

Transmittance measurements have been made on single-crystal $\text{Y}_{1-x}\text{Pr}_x\text{Ba}_2\text{Cu}_3\text{O}_6$ ($x = 1., 0.4, 0.$) in the frequency range between 700 and 4000 cm^{-1} , in magnetic fields (B_0) up to 30 T, and at temperatures between 5 K and 400 K. Absorption features that have been ascribed to magnon excitations in the CuO_2 planes are very insensitive to the applied field. The substitution of Pr^{3+} for Y^{3+} leads to an additional absorption feature, which does have a strong field dependence. The behavior is almost independent of the concentration x and is controlled by the field component $B_0 \parallel c$. This excitation process is assigned to an intermultiplet transition in the Pr^{3+} ion. The zero-field temperature dependence of this absorption shows clear evidence of an interaction between Cu and Pr spins.